Organic & Biomolecular Chemistry

ROYAL SOCIETY OF CHEMISTRY

PAPER

View Article Online
View Journal | View Issue

Cite this: *Org. Biomol. Chem.*, 2025, **23**, 4983

Domino synthesis of a new class of red-shifted and antimicrobial imidazole-based azo dyes from 5-aminoimidazole-4-carboxamidrazones†

Mariana P. Silva, [a] Bárbara Silva,[b,c] Inês Costa,[b,c] Paulo J. G. Coutinho, [d] Fátima Cerqueira,[e,f,g] Eugénia Pinto[h,i] and Alice M. Dias *[a]

Received 15th March 2025,
Accepted 22nd April 2025

DOI: 10.1039/d5ob00463b

rsc.li/obc

Combining antimicrobial activity with halochromic properties offers an enticing opportunity to both combat and detect microbial infection in the medical field. Previous research has identified a class of compounds that demonstrate potent antimicrobial activity, particularly against pathogenic yeasts. Notably, these compounds also exhibit vibrant pink–blue colours and a halochromic behaviour within the therapeutic pH range. Aiming at developing a more sustainable synthetic method and to generate better red-shifted and pH-responsive imidazole-based azo dyes, a new domino reaction was discovered yielding a novel class of green-coloured 2-aminoimidazole azo-dyes. A strategy based on circular chemistry was achieved by introducing the accessible and environmentally benign O_2/KI oxidant system, which is able not only to regenerate the oxidants but also minimize side reactions. The isolation of two key intermediates was also an important achievement in comprehending the underlying mechanisms. As expected, this new class of 2-aminoimidazole dyes also presented significant solvatochromism and pronounced halochromism with colours changing from green to purple as the pH decreases. *Ab initio* molecular quantum mechanics calculations supported the data obtained experimentally. A great number of compounds (12 in 18 compounds) showed potent fungicidal activity against *C. neoformans* and moderate activity against *C. krusei*.

1. Introduction

Infections caused by pathogenic fungi affect more than a billion people worldwide, and invasive fungal infections are responsible for higher mortality rates and result in higher death tolls than tuberculosis or malaria.[1] The majority of these deaths are caused by pathogenic fungi of the genus *Candida*, *Cryptococcus*, *Pneumocystis*, and *Aspergillus*.[2] As mycoses are one of the major causes of morbidity/mortality among immunocompromised individuals, the World Health Organization (WHO) defined a fungal pathogens priority list to guide research development, and public health action. The list includes *Candida albicans*, *Cryptococcus neoformans* and *Aspergillus fumigatus* in the critical priority group while *Pichia kudriavzevii* (*Candida krusei*) is included in the medium priority group.[3]

Nonetheless, the increased resistance to antifungal drugs of non-*albicans Candida* (NAC) species, including *C. krusei*, is changing the epidemiology of candidiasis. In addition, *C. krusei* can cause life-threatening infections in patients with hematologic malignancies and immune-compromised individuals, with a higher risk in cases of prolonged azole prophylaxis.[2] Among the predominant fungi impacting human

[a]*Centre of Chemistry of University of Minho (CQ-UM), Department of Chemistry, University of Minho, Campus de Gualtar, 4710-057 Braga, Portugal. E-mail: ad@quimica.uminho.pt*
[b]*Associate Laboratory i4HB—Institute for Health and Bioeconomy, Faculty of Pharmacy, University of Porto, 4050-313 Porto, Portugal*
[c]*UCIBIO—Applied Molecular Biosciences Unit, Laboratory of Toxicology, Department of Biological Sciences, Faculty of Pharmacy, Porto University, 4050-313 Porto, Portugal*
[d]*Physics Centre of Minho and Porto Universities (CF-UM-UP) and LaPMET (Laboratory of Physics for Materials and Emergent Technologies), Campus de Gualtar, 4710-057 Braga, Portugal*
[e]*FP-I3ID, FP-BHS, GIT-LoSa, University Fernando Pessoa, Praça 9 de Abril, 349, 4249-004 Porto, Portugal*
[f]*Faculty of Health Sciences, University Fernando Pessoa, Rua Carlos da Maia, 296, 4200-150 Porto, Portugal*
[g]*Molecular Oncology and Viral Pathology Group, Research Center of IPO Porto (CI-IPOP)/RISE@CI-IPOP (Health Research Network), Portuguese Oncology Institute of Porto (IPO Porto)/Porto Comprehensive Cancer Center (Porto.CCC), Porto, Portugal*
[h]*CIIMAR/CIMAR, Interdisciplinary Centre of Marine and Environmental Research, Terminal de Cruzeiros do Porto de Leixões, 4450-208 Matosinhos, Portugal*
[i]*Laboratory of Microbiology, Biological Sciences Department, Faculty of Pharmacy of University of Porto, 4050-313 Porto, Portugal*

† Electronic supplementary information (ESI) available. See DOI: https://doi.org/10.1039/d5ob00463b

health, *C. neoformans* show alarming statistics with a global burden of cryptococcal meningitis of 250 000 cases/181 000 deaths annually, and involving a mortality rate of 100% for untreated infections.[1,4] Moreover, treatment options for cryptococcosis are more limited, as *Cryptococcus* spp. has an inherent resistance to echinocandins.[1]

The few currently available antifungal drugs for invasive fungal infection treatments are limited to polyenes, azoles and echinocandins. However, their high host toxicity, the acquired fungal resistance, and the advent of other species with a broader resistance spectrum raise the need for new molecules that combine enhanced fungicidal activity with lower host toxicity while being capable of evading common resistance mechanisms.[24,25]

Chemical production faces major problems with the handling of waste, large expenses and reduction of resources, as well as inefficient processes.[5] These problems require solutions that would not only be more environmentally friendly but also reduce resource consumption and cut production costs. Domino reactions (also known as cascade or Tandem reactions) are extremely beneficial to synthetic chemists as chemical conversions are sequential reactions occurring in the same reaction vessel, and products of one reaction are substrates for the next sequential reaction step. The benefits over the usual stepwise formation of the individual bonds include a high atom economy and a more streamlined process. In addition, the replacement of the expensive and toxic chemicals with environmentally benign reagents/catalysts and synthesis design closer to the principles of the circular economy aligns with sustainability principles while benefiting chemical production.[6]

Azobenzenes stand out concerning their colouring ability, which inspired the synthesis of a wide range of azo dyes with a myriad of applications including dyeing of natural and synthetic materials, medicine, inks, cosmetics, food and paints.[7] The classical method to obtain azo dyes is a two-step pathway involving diazotisation and coupling reactions with electron-rich aromatic species.[7,8] The azobenzene chromophore absorbs radiation in the visible region, around a wavelength of 450 nm (molar absorption coefficient (ε) $\approx$ 400 L mol^{-1} cm^{-1}), due to a n–π^* transition from the ground state (S0) to the first singlet excited state (S1), and in the ultraviolet (UV) region, around a wavelength of 300 nm (molar absorption coefficient (ε) $\approx$ 22 000 L mol^{-1} cm^{-1}), due to a π–π^* transition to the second excited state (S2).[7,9–12] In the aminoazobenzenes, electron-donating amino groups at the 4-position, or further substitution with cyano or nitro groups, respectively, lead to a bathochromic shift that brings together the π–π^* and n–π^* bands.[7] Aminoazobenzenes also display halochromic properties, meaning they are sensitive to pH and undergo visible colour change upon pH variation. If protonation occurs in the nitrogen of the azo-group, a bathochromic shift occurs, while a protonation at peripheral nitrogens causes a hypsochromic shift.[13] Typically, an equilibrium between ammonium and azonium ions is established, where each of these two tautomeric forms originates a different absorption band and exhibits a different colour.[14]

Red-shifted azobenzenes are promising candidates for use in photopharmacology as they exhibit photo-responsive signals within the spectrum of visible light,[10] thereby avoiding the harmful side effects of UV radiation. These compounds can be obtained by three main strategies that involve push–pull systems,[7,15] bridged azobenzenes,[7] and *ortho*-substituted azobenzenes with two amino,[16] two *ortho*-methoxy,[17] two *ortho*-fluorine groups,[18] or tetra-*ortho*-methoxy substituents.[19–23]

The addition of heterocyclic moieties to azobenzenes opens a new world of possibilities regarding their photophysical, chemical, and biological properties.[24] Arylazoimidazoles, the second most utilized and studied heteroaryl azo-dyes after azopyridines,[25,26] are a pivotal example of the hydrazone tautomerism mechanism, and may act as bases due to the basic nitrogen atom in the imidazole ring. Similarly to other azobenzenes, the classical synthetic route for azoimidazoles is diazotization of the aromatic or heterocyclic amine, followed by coupling of the diazonium salt with a nucleophile segment (Scheme 1A).[27–29]

Imidazoles are one of the most promising classes of contemporary antifungal agents. Showing broad spectrum and potent activity, excellent bioavailability, good tissue penetrability and permeability and a relatively low incidence of adverse and toxic effects, they have been found effective in the treatment of various infectious diseases.[4] In addition, the 2-aminoimidazole moiety is an extremely useful building block for the design of small-molecule drugs as modulators of different targets.[30] The methods for obtaining this moiety are the condensation of α-aminoketones or α-aminoaldehydes with cyanamides, or α-haloketones with guanidine derivatives; and the reaction between propargylic amines and carbodiimides,[31] but expensive catalysts, harsh conditions and availability of reagents are still major limitations of these methods. The

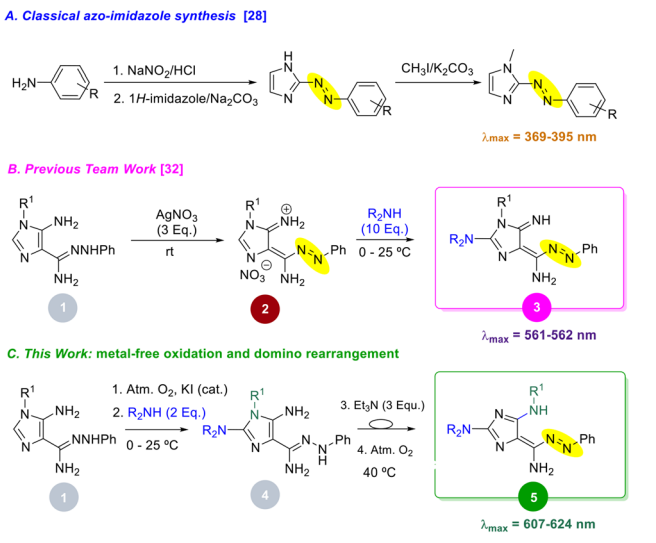

Scheme 1 (A) Classical azoimidazole synthesis still used; (B) previously developed pathway for the synthesis of azoimidazoles **3** from amidrazone-based imidazole precursors **1**; (C) and synthesis of the new azoimidazoles **5** here presented.

alternative functionalization of imidazole derivatives also requires multiple steps, protection/deprotection strategies, and activation of C-2 for the introduction of the amine.

Previous findings of our group led us to obtain a novel class of 2-aminoimidazole azo dyes (**3**) from Ag^{+}-mediated oxidation of imidazole-based amidrazones **1**, followed by the addition of secondary amines to the azo intermediates **2**, generating the 2-aminoimidazole skeleton (Scheme 1B).[32] These unique azo-dyes (**3**) exhibited unusual red-shifted absorption bands, and significant halochromism near the physiological pH with the vibrant magenta (neutral form) changing to a deep blue (protonated form) colour. They also demonstrated potent antimicrobial properties against infectious yeasts (minimum inhibitory concentration (MIC) ≈ 4 μg mL^{-1} for *C. krusei*), and no cytotoxicity was detected for concentrations lower than 16 μg mL^{-1}.[32] The halochromism near the physiological pH, as well as the promising antifungal activity, allowed the development of (bio)medical and textile applications.[33,34]

Despite the previous method (**B**) being simple and fast at mild conditions, a large excess of the secondary amine is required to prevent degradation events and the formation of unwanted secondary products. Moreover, stoichiometric amounts of the expensive silver nitrate were required, and an additional purification step is mandatory to remove the metallic Ag^{0}. On the search for greener catalysts and more sustainable conditions, we found a novel class of 2-aminoimidazole-based azo-dyes **5** (Scheme 1C) that showed an absorption band even more red-shifted than the previous azo-dyes **3**, exhibiting a vibrant green colour that changes to purple upon protonation. These azo-dyes also showed moderate-strong activity against *C. krusei* and potent activity against *C. neoformans.*

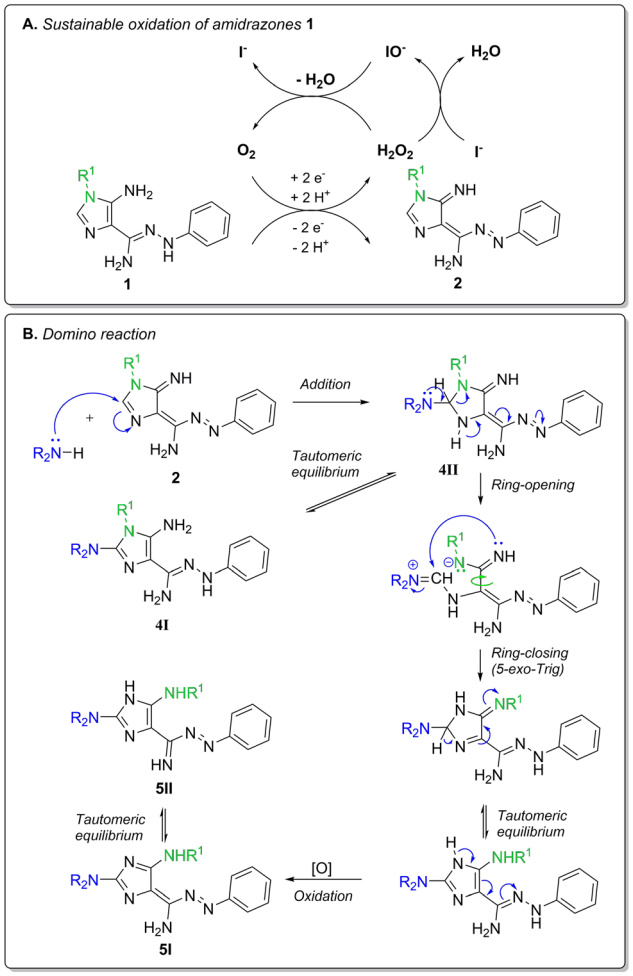

Scheme 2 Proposed reaction mechanism for the synthesis of azoimidazoles **5** from amidrazone precursors **1**.

2. Results and discussion

2.1. Synthesis

The first objective of our recent research was to replace silver nitrate with a more sustainable oxidant. Preliminary attempts to replace silver nitrate by atmospheric air evidenced a fast reaction with the production of hydrogen peroxide, but degradation and formation of unwanted secondary products were still major drawbacks. As hydrogen peroxide has been associated with the breakdown of the N=N bonds, leading to degradation of the azo chromophore,[35] preliminary investigations of the stability of our azo dyes in the presence of hydrogen peroxide were conducted. Results evidenced a fast loss of colour, suggesting the reduction of the azo bond possibly followed by fragmentation reactions. These results led us to explore the use of potassium iodide (KI) to promote the cyclic decomposition of hydrogen peroxide (H_2O_2) and the *in situ* generation of O_2, according to Scheme 2A.

Various amidrazones **1** were reacted with piperidine in the presence of KI, and it was found that amidrazones with aromatic substituents at the N^1-position (R^1 = aryl) enabled to isolate solid mixtures with a dark green colour (Table 1). NMR data of these mixtures was not sufficient to shed light on the structure of the products, but chemical shifts of the observed phenyl groups revealed the presence of two amidrazones and two azo compounds. One of the amidrazones was assigned to the starting reagent (**1**), but the other three compounds contained piperidine units, as three sets of methylenic $N(CH_2)_2$-protons were identified. These compounds were later identified as compounds **4I**, **4II** and **5**.

Once the fast formation of azo-dyes in the sustainable O_2/KI oxidation system was demonstrated, finding the ideal mixture of solvents that led to complete the consumption of amidrazone **1** was crucial, and it was found that the mixture of acetonitrile/water (2 : 1) resulted in superior yields. Then, several attempts were performed to find the appropriate concentrations of KI and piperidine. It was concluded that only catalytic quantities of KI were needed and two equivalents of piperidine were sufficient to guarantee the success of the reaction, unlike the ten equivalents required in the synthesis of the azo-dyes **3**. Temperature also played an essential role in reaction rate and selectivity, and it was possible to successfully isolate three intermediates **4** in the pure form by lowering the reaction temperature to 0 °C. Full characterization of these

Table 1 Optimization of the synthesis of azoimidazoles **5**

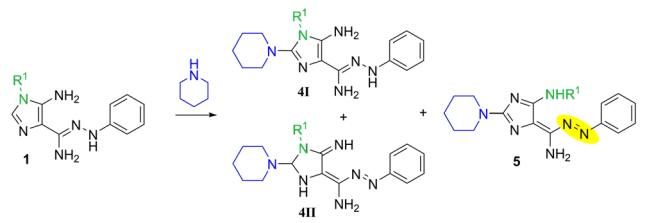

Starting reagent	Reagents	Solvents	Temp. (°C)	Products (^{1}H NMR)	Yield (%)
1e	2 eq. Pip	H_2O/ACN (2 : 1)	25	**4i_I** (36%)	[a]
	3 eq. KI			**4i_II** (14%) **5i** (50%)	
1e	2 eq. Pip 3 eq. KI	ACN	25	**5i** (100%)	34
1e	3 eq. Et_3N 2 eq. Pip 0.2 KI	H_2O/ACN (1 : 2)	25	**5i** (100%)	77
1e	2 eq. Pip	H_2O/ACN (1 : 2)	25	**5i** (90%)	[a]
	3 eq. KI			Unwanted products (10%)	
1f	2 eq. Pip 3 KI	H_2O/ACN (1 : 2)	0	**4j_I** (100%)	67
4j	3 eq. Et_3N	ACN	40	**5j** (100%)	47
4j	3 eq. Et_3N	ACN	40	**5j** (100%)	46

[a] Yield was not calculated due to the presence of a complex mixture.

intermediates was not possible due to their unstable nature, as they promptly evolve to the final azo-dyes **5** when maintained in solution. However, structures of tautomer **4I** could be assigned with significant confidence based on the data obtained from ^{1}H, ^{13}C NMR and 2D (HSQC and HMBC) spectroscopy. For tautomer **4d_II**, although the isolation was also possible, its evolution in DMSO-d_6 was so fast that it only allowed to infer its structure by comparison of the ^{1}H NMR spectra of the two tautomers (**4I** and **4II**). Both compounds present a phenyl group, but major noticeable differences exist. **4II** shows an azo-like structure as the *ortho* protons of the aza phenyl group (N=NPh) appear at δ 7.25–7.26 ppm (doublet), while **4I** presents the corresponding *ortho* protons of the phenylhydrazone group (C=N–NHPh) at δ 6.80–6.82 ppm, revealing an amidrazone-like structure. This was also deduced based on the presence and relative position of the NH and NH_2 groups. For instance, **4II** presents only one NH_2 signal (δ 6.09–6.10 ppm) and two NH signals (the imino group at δ 9.11–9.12 ppm, and the imidazole NH at δ 9.26–9.37 ppm). In contrast with this, **4I** shows two NH_2 signals (δ 5.21–5.39 ppm and δ 5.60–5.65 ppm) and only one NH signal belonging to the phenylhydrazone unit (δ 7.84–7.89 ppm). Another significant and easily identifiable difference is the presence of a CH signal in **4II**, whose proton appears as a singlet at δ 6.39–6.42 ppm, which is typical of a proton bonded to a sp^3 carbon with two nitrogen neighbours. The presence of this tetrahedral carbon was also confirmed by ^{13}C NMR spectroscopy as it appeared at δ 95.9 ppm and showed a direct correlation with the proton at δ 6.39–6.42 ppm, in the HSQC spectrum. Moreover, the two forms can be distinguished by the relative position of piperidine, which presents a chemical shift of δ 2.55–2.56 ppm in **4II** and δ 2.77–2.78 ppm in **4I**.

When intermediates **4i** reacted under atmospheric oxygen, the evolution to coloured products was fast, but contamination of azo-dyes **5** with traces of unwanted products was a limitation of the method (Table 1). These drawbacks led to optimising conditions by investigating the effects of increasing reaction temperature, as well as the presence of acid or base catalysts. When triethylamine was introduced in the reaction mixtures and the temperature was increased to 40 °C, products **5** were isolated pure. However, the additional step of isolating the intermediates **4** led to lower yields. As such, to prevent this issue, the sequential synthesis of **5i** from amidrazones **1** and piperidine in a one-pot two-step method was attempted with success. These new conditions proved to be reproducible, including when different secondary amines were used (dimethylamine and pyrrolidine), allowing the isolation of eighteen azo-imidazoles **5** (Table 2) and demonstrating the versatility of the method.

This new class of azoimidazoles was characterized by ^{1}H and ^{13}C NMR spectroscopy. As azobenzene derivatives, these compounds contain a phenyl group, which was identified due to the presence of the aromatic protons at δ 7.40–7.72 ppm and the corresponding carbon atoms appearing at δ 152.8–121.4 ppm, identified by HMBC NMR spectroscopy. The core imidazole of this structure exhibits C-2, C-4 and C-5 signals that compare with the previous series of azo-dyes **3**. However, the presence of the second sp^2 nitrogen atom in the imidazole ring must be responsible for the observed shift of *ca.* 10 ppm to the lower field of C-2 signal (δ 169.0–171.9 ppm), as demonstrated by the three-bond HMBC correlation with the methylenic/methylic protons of the secondary amine moiety. Proton signals of this 2-amino substituent were also shifted to higher chemical shift values, as confirmed by the broad singlets (4H) at δ 3.88–3.89 ppm for piperidino, and δ 3.72–3.75 ppm for pyrrolidino, as well as the singlet (6 H) at δ 3.32–3.33 ppm for dimethylamino groups. C-4 signal is also shifted in the same direction (δ 136.7–137.5 ppm). The C-5 signal appears at δ 164.1–164.7 ppm and was assigned through correlations with the 5-NH proton (two-bond correlation) and the protons of C_o of the R^1 group's aromatic ring (four-bond correlations).

As proposed in Scheme 2, this reaction begins with the oxidation of amidrazone **1** to afford azoimidazole **2** in the presence of an O_2/KI system (Scheme 2A). Once formed, this azoimidazole suffers a fast nucleophilic attack of the secondary amine to the C-2 carbon atom of the imidazole core (Scheme 2B). This attack weakens the structure of the imidazole core and allows a ring-opening reaction, which is favoured by the presence of the aromatic substituent because the negative charge developed will be particularly delocalized

Table 2 Synthesis of a new class of azoimidazoles (**5**)

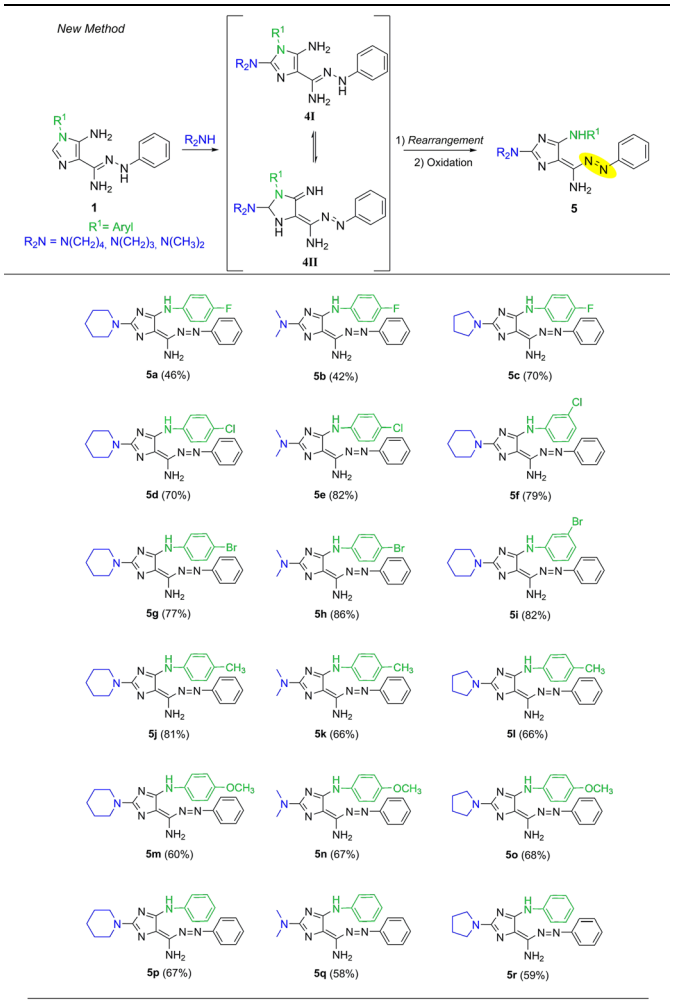

Reaction conditions: to a suspension of amidrazones **1** in acetonitrile (2 mL) and water (1 mL), triethylamine (3 molar eq.), a secondary amine (piperidine, dimethylamine or pyrrolidine; 2 molar eq.) and KI (0.2 eq.), were added under magnetic stirring. After 4–5 hours at 40 °C, the products were filtrated with water, acetonitrile and diethyl ether, under nitrogen.

over the benzene ring. A rotation of the C4–C5 bond occurs, enabling the ring-closing by a nucleophilic attack of the NH group to the activated amidine group through a 5-*exo-trig* cyclization. This is the key step of this rearrangement that essentially causes the NR^1 and NH groups to shift their positions when the imidazole ring is rebuilt. In the next steps, the tautomeric equilibria established must be shifted towards a more stable structure, restoring the aromaticity to the imidazole core of the target compound. Finally, an oxidation step results in the final azoimidazoles **5**.

3. Photophysical characterization

The UV-Vis spectra of compounds **5** were obtained from 350 nm to 700 nm in ethanol, acetonitrile and 1,4-dioxane. The maximum absorption wavelength and molar absorption coefficients were also determined. Azoimidazoles **5** present two distinct bands in the visible region of the spectrum: one band around 413–441 nm, corresponding to an absorption in the purple region, and another band around 604–633 nm, corresponding to an absorption in the yellow-orange region of the spectrum. The complementary colours of purple and orange are, respectively, yellow and blue, which, when combined, explain the green colour presented by compounds **5**. These compounds present molar absorption coefficients of 1.15–5.12 × 10^4 M^{-1} cm^{-1}, regarding their main absorption band.

In ethanol, all compounds present a similar position of the absorption bands, except **5j** and **5m** (R^1 = $C_6H_4(p)CH_3$ and R^1 = $C_6H_4(p)OCH_3$), which show a red-shift in both bands (Fig. 1). This could be related to the presence of an electron-donating group in the aromatic ring. When it comes to the intensity of the main absorption band, the presence of halogens in the substituent seems to be directly linked to a hyperchromic effect, which is more pronounced in **5g** (R^1 = $C_6H_4(p)Br$) There is also a significant hypochromic effect presented by **5m** (R^1 = $C_6H_4(p)OCH_3$).

Regarding R^2-substituents, there is no discernible pattern, as the relative absorbance of the different compounds varies depending on the R^1-substituent. For instance, when R^1 = $C_6H_4(p)CH_3$, the compound containing a pyrrolidine unit shows higher absorbance throughout all wavelengths, followed by the piperidino-substituted compound. However, when R^1 = $C_6H_4(p)OCH_3$, the compound presenting the piperidine moiety presents a significantly lower absorbance than its counterparts.

When it comes to solvatochromism, hypsochromic shifts are observed when increasing solvent polarity in the sequence 1,4-dioxane; acetonitrile; ethanol. The difference between λ_{max} values in ethanol and acetonitrile is 5 to 9 nm, while between acetonitrile and dioxane, it is only 1 to 5 nm. Fig. 2 presents the spectra of **5a** (R^1 = $C_6H_4(p)F$) in each solvent to illustrate

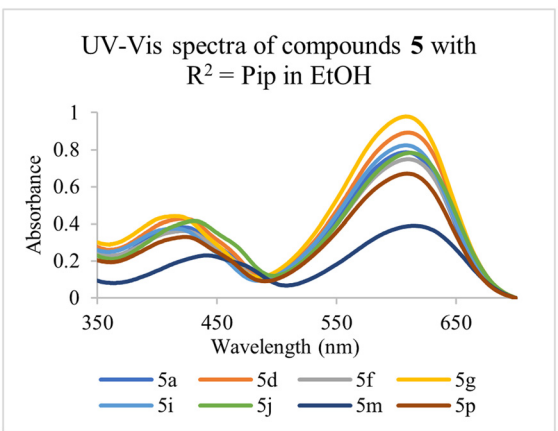

Fig. 1 UV-Vis spectra of compounds **5** with R^2 = Pip in ethanol with varying R^1 substituents, at 3.33 × 10^{-5} M.

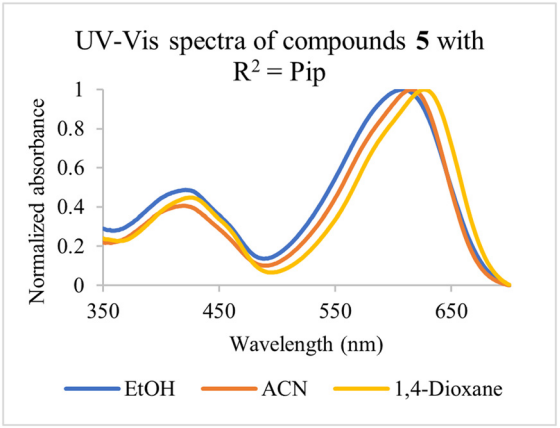

Fig. 2 Normalized UV-Vis spectra of **5a** in ethanol, acetonitrile and 1,4-dioxane, at 3.33 × 10^{-5} M.

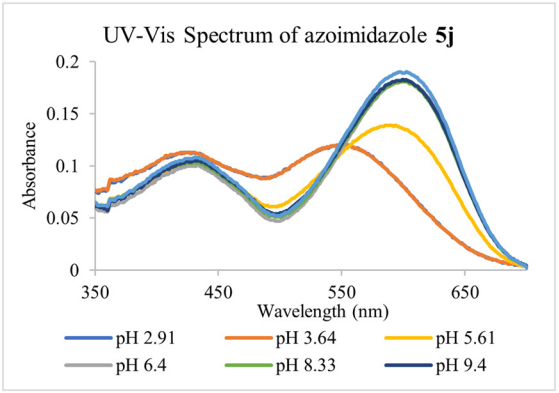

Fig. 4 UV-Vis spectra of azoimidazole **5j at different pH values** in water/ethanol (60 : 40), and at 10^{-5} M. A pH electrode was used to determine pH values.

the shift caused by these solvents, which is similar in all compounds. When it comes to the band around 430 nm, it is difficult to identify a pattern in the effects of the R^1-substituents, but there is solvatochromism, particularly between compounds in acetonitrile and 1,4-dioxane solutions.

To demonstrate the halochromic properties of these molecules, the UV-Vis spectra of compound **5j** were obtained from 350 nm to 700 nm, before and after adding 1 molar equivalent of sulfuric acid to a solution with a concentration of 4 × 10^{-5} M in ethanol (Fig. 3).

In its neutral form, **5j** presents two distinct bands at 432 nm and 597 nm that result in the transmittance of the green colour. The acid form of this compound also presents two bands. The first, at 427 nm, shows a slight bathochromic shift. The second band, at 552 nm, suffers the most significant difference in both position and intensity. More specifically, there is a 45 nm hypsochromic shift into the yellow region that almost halves the absorbance value, explaining why this compound exhibits a colour in the purple region, as these two colours are complementary.

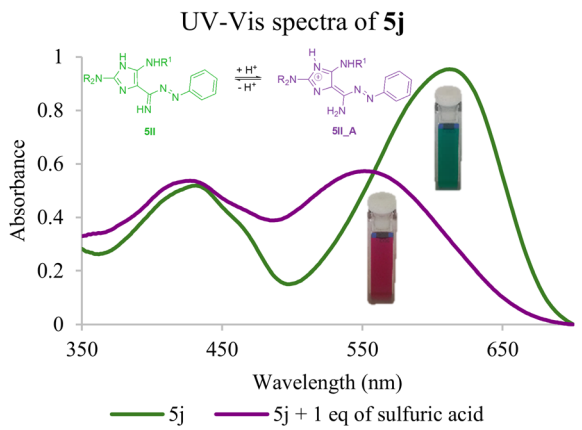

Fig. 3 UV-Vis spectra of azoimidazole **5j** in ethanol at 4 × 10^{-5} M, before and after adding 1 molar equivalent of sulfuric acid, including photographs of the two forms.

A more comprehensive study was also conducted, in which UV-Vis spectra of compound **5j** were traced between 350 and 700 nm at different pH values, measured with a pH electrode (Fig. 4). This allowed the determination of pK_a, using the graphical method reported by Salgado *et al*. The obtained pK_a value was 4.89.

In order to further understand the photophysical behaviour of this compound, molecular quantum mechanical calculations were performed for compound **5k** in ethanol. As various tautomers are possible, ground state geometry optimization and vibrational analysis were obtained for various possible tautomers, ensuring that no imaginary frequency modes were present. Within an energy difference of 15 kcal mol^{-1}, five structures were found (ESI-Table 3†). Using TDDFT with the b3lyp functional, vertical electronic excitation energies were then obtained for the first eight excited states. Comparing with the experimental maximum wavelengths in ESI-Table 1† the tautomer with lowest energy (I) is significantly to the blue. This shift is not explainable by the used functional as it normally originates smaller excited state transition energies. Although being 14.6 kcal mol^{-1} more energetic, tautomer II shows bands at 436 nm and 701 nm with significant intensity, as seen from the oscillator strength values (f_{osc}), that are more compatible with the observed experimental spectrum. Looking for possible mechanisms to explain the possible prominence of tautomer II, calculations were performed in the presence of one explicit water molecule (ESI-Table 4†). Hydrogen-bond type interaction was found and the excess energy of tautomer II decreased to 10 kcal mol^{-1}. Additionally, the electronic transition energies and relative oscillator strengths became more compatible with the experimental spectrum. From these parameters an absorption spectrum can be calculated assuming Gaussian bands with 0.2 eV standard deviation. Transforming it in transmitted light and using the CIE colour matching functions it is possible to predict a corresponding perceived human colour. ESI-Fig. 10† shows a green colour for tautomer II confirming its importance. The nature of the electronic excitations can be inferred from the

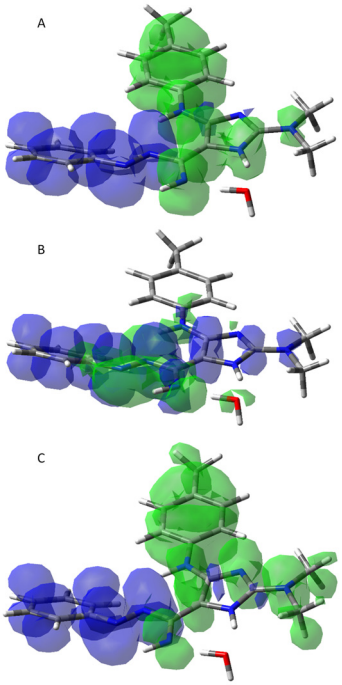

Fig. 5 Electron density variation upon excitation to first (A) second (B) and third (C) excited states of compound **5k** + H_2O in ethanol. Green and blue areas correspond to decrease and increase of electron density.

variations of electron density upon excitation. These are represented in Fig. 5. In the first and third electronic transitions, variations of electron density occur mainly at the π electron cloud perpendicular to the molecular plane, indicating them to be of type π–π*. On the contrary, in the second electronic transition electron density decreases in the nitrogen atoms along the molecular plane and increases in the π electron cloud. This behaviour is typical of an n–π* type transition and justifies its lower oscillator strength.

Calculations were also performed for protonated forms of both tautomer **5k_I** and **5k_II** (ESI-Table 5†). Protonation free energies were calculated assuming 0.4 kcal mol^{-1} (1050.2 kJ mol^{-1}) for the free energy of the proton in ethanol.[36] From the protonated form with lowest protonation free energy (II_A) a pK_a value of 4.95 can be calculated, which is in very good accordance with determined value for compound **5j**. Colours for the protonated forms of tautomer **5k_II** are also shown in Fig. ESI-10† and again a very good match is obtained for protonated form **5k_II_A**.

4. Antimicrobial activity

The antifungal and antibacterial activity of the newly synthesised compounds were evaluated (Table 3 and ESI-Table 6†). From the eighteen compounds tested, twelve derivatives showed potent activity against *C. neoformans* (MIC between 2–20 μg·mL^{-1}), with compound **5j** showing the best results. For *Candida* spp., seven compounds showed significant antifungal activity against *C. krusei* (MIC between

Table 3 Minimum inhibitory and lethal concentrations of compounds **5** featuring superior antimicrobial potential[a]

	MIC (MLC) μg mL^{-1}		
	5j	**5b**	**5k**
C. albicans ATCC 10231	89.6 (≥256)	192± (213.3)	256 (256)
C. krusei ATCC 6258	4.0 (5.3)	13.3 (13.3)	16 (16)
C. neoformans CECT 1078	2.0 (3.3)	8 (13.3)	7.3 (13.3)
T. rubrum FF5	44.0 (48.0)	128 (128)	128 (128)
S. aureus ATCC 25923	10.7 (≥256)	64 (>256)	>256 (>256)

[a] Full results in ESI;† MIC/MLC, minimum inhibitory/lethal concentration.

4–20 μg·mL^{-1}) and nine compounds showed moderate activity (MIC between 20–80 μg·mL^{-1}). The compounds showed greater selectivity for *C. krusei*, considering that the MIC values for *C. albicans* were higher than 256 μg·mL^{-1} for the majority of the compounds and the best was 89.6 μg·mL^{-1} albeit being fungistatic. Minimum lethal concentration (MLC) values for *C. neoformans* and *C. krusei* were identical to the MIC values (equal or one dilution higher), which represents an interesting fungicidal activity for these compounds against these species. Concerning filamentous fungi, some fungicidal activity was observed for some compounds on the dermatophyte *T. rubrum*, but for *A. fumigatus* all the compounds showed a MIC value ≥256 μg·mL^{-1}, the maximum concentration tested (ESI Tables 3 and 4†). Concerning the antibacterial activity, only compound **5j** showed good activity against *Staphylococcus aureus* with a MIC value of 10.7 μg·mL^{-1}. However, the effect was bacteriostatic and not bactericidal as with *C. neoformans* and *C. krusei*. Some selectivity against Gram-positive bacteria was revealed, as no compound showed any activity against *Escherichia coli*.

5. Conclusions

A sustainable and efficient method for the synthesis of a new class of 2-aminoimidazole azo-dyes with remarkable colorimetric, halochromic and antimicrobial properties was developed. The introduction of the O_2/KI oxidation system in the synthesis pipeline as an alternative to silver nitrate was an innovative strategy that allowed the efficient and sustainable synthesis of various azoimidazoles **5**. This is an entirely different class of azoimidazoles, when compared with classical azoimidazoles. However, they show some structural similarities with the 2-aminoimizole azo-dyes series previously reported by our group **3**. The study of the mechanism involved in the synthesis of these unexpected green solids led to the isolation of the intermediate compounds **4I** and **4II**. A total of eighteen green solids were isolated and characterized by ^1H, ^{13}C and 2D NMR spectroscopy, infrared spectroscopy, and elemental analysis.

The original 2-aminoimizole azo-dyes **3** presented unique properties, such as halochromism and antimicrobial activity,

and these properties were also studied for this new azo-dyes (**5**). Interesting solvatochromism was found in azoimidazoles **5**, with the highest shift in maximum wavelength of absorbance being found for **5** with R^2 = Pyr. All 2-aminoimidazoles **5** presented a molar absorption coefficient around 10^4 M^{-1} cm^{-1}. Protonation studies indicated the presence of halochromism in compounds **5**, with their colours changing from green to purple when the pH decreases. *ab initio* molecular quantum mechanics calculations support the data obtained experimentally.

Data from the conducted antimicrobial activity assays evidences good antimicrobial activity of the newly synthesised 2-aminoimidazoles **5** against pathogenic yeasts. The majority of the tested derivatives showed potent activity against *C. neoformans*, and moderate activity against *C. krusei*. Compound **5j** was the best hit compound for both *C. neoformans* (MIC = 2 $\mu g \cdot mL^{-1}$) and *C. krusei* (MIC = 4 $\mu g \cdot mL^{-1}$). The data also suggest that the antifungal activity was fungicidal and selective for these two species. These results are interesting since *C. neoformans* is responsible for a high mortality rate among infected individuals and drug resistance is an actual problem, while *C. krusei* is intrinsically resistant to fluconazole but is also able to develop acquired resistance to other azoles.

Altogether, the new azo-dyes **5** stand as promising candidates for the development of new compounds for (bio)medical applications.

6. Experimental

6.1. Materials and instruments

All new compounds were fully characterized by NMR (^1H, ^{13}C) on a Bruker Avance 3400 (^1H: 400 MHz, ^{13}C: 100 MHz), including the ^1H–^{13}C correlation spectra (HMQC and HMBC) using DMSO-d_6 as solvent at room temperature or 50 °C. The coupling constants (J) are reported in Hertz (Hz) and chemical shifts (δ) were expressed in parts per million (ppm). IR spectra were recorded on a FT-IR Spectrum Two – PerkinElmer, at room temperature in the range of 4000–450 cm^{-1}. Melting points were determined on a Stuart cat. SMP3 and are uncorrected. The reactions were monitored by TLC analysis, performed in Merck-Kieselgel 60 F254 silica plates and observed in a CN-6 ultraviolet light (ν = 50 Hz) chamber. UV-Vis spectra were obtained with UV-2501PC by Shimadzu Corporation, using 1 cm wide quartz cells. Elemental analysis data were obtained with the analyser Leco TruSpec CHNS Micro.

6.2. *Ab initio* molecular quantum mechanics calculations

The electronic and structural properties of compound **5k** were studied by *ab initio* molecular quantum chemistry calculations through orca software version 6.0.1 [37] with a def2-TZVP[38] basis set using the DFT method and RIJCOSX approximation[39] using def2/J[40] as auxiliary basis. The B3LYP functional was used together with atom-pairwise dispersion correction based on EEQ partial charges (D4)[41] and a conductor-like polarizable continuum model (CPCM) corresponding to ethanol. Excited state calculations were done through time-dependent DFT using the Tamm-Dancoff approximation (TDDFT-TDA).[37] For the case of interaction with an explicit water molecule geometrical counter-poise correction (gCP) was used to correct artificial overbinding effects that can arise from basis set superposition error (BSSE).[42]

6.3. Synthesis

6.3.1. General procedure for the synthesis of 5-aminoimidazole-4-carboxamidrazones 1. The general procedure to obtain amidrazones **1** followed a method previously developed by the research group.[43] To a suspension of 5-amino-4-(cyanoformimidoyl)-1*H*-imidazole (1.7–4.4 mmol) in ethanol (2–7 mL), phenylhydrazine (1.5–2.0 molar equivalents) and catalytic quantities of acetic acid (5–10 μL) were added, under magnetic stirring. The reaction mixture was placed in an ice bath under nitrogen purge for 10 minutes. The suspensions were stirred at 8 °C for 4–26 h until the reactions were completed according to a TLC in DCM/EtOH (9 : 1), presenting R_f values ranging from 0.41 to 0.73. At this point a filtration was performed with ethanol and diethyl ether and the pure amidrazones **1** were obtained.

6.3.2. (*Z*)-5-Amino-1-(4-fluorophenyl)-*N*′-phenyl-1*H*-imidazole-4-carbohydrazonamide (1a). 5-Amino-1-(4-fluorophenyl)-1*H*-imidazole-4-carbimidoyl cyanide (1.00 g, 4.4 mmol), ethanol (3 mL), phenylhydrazine (0.693 mL, 7.0 mmol) and acetic acid (10 μL). After 6 hours at 8 °C, compound **1a** was obtained pure (0.927 g, 2.9 mmol, 68%). M.p. > 156 °C (dec.). ^1H NMR (400 MHz, DMSO-d_6): 5.67 (brs, 2H), 5.80 (brs, 2H), 6.58 (t, J = 7.2 Hz, 1H), 6.85 (d, J = 7.6 Hz, 2H), 7.12 (t, J = 8.0 Hz, 2H), 7.40 (s, 1H), 7.41 (t, J = 8.8 Hz, 2H), 7.60 (dd, J = 9.2 Hz, J = 4.4 Hz, 2H), 7.94 (s, 1H). ^{13}C NMR (100 MHz, DMSO-d_6): δ 111.6, 113.7, 116.4, 116.6, 126.7 (d, J = 8 Hz), 128.7, 129.0, 131.5 (d, J = 3 Hz), 136.8, 145.0, 147.9, 161.2 (d, J = 243 Hz) ppm.

6.3.3. (*Z*)-5-Amino-1-(4-chlorophenyl)-*N*′-phenyl-1*H*-imidazole-4-carbohydrazonamide (1b). 5-Amino-1-(4-chlorophenyl)-1*H*-imidazole-4-carbimidoyl cyanide (1.00 g, 4.1 mmol), ethanol (7 mL), phenylhydrazine (0.602 mL, 6.2 mmol) and acetic acid (10 μL). After 26 hours at 8 °C, compound **1b** was obtained pure (1.11 g, 3.4 mmol, 83%). M.p. > 182 °C (dec.). ^1H NMR (400 MHz, DMSO-d_6): δ 5.72 (brs, 2H), 5.80 (brs, 2H), 6.58 (t, J = 7.2 Hz, 1H), 6.84 (d, J = 7.6 Hz, 2H), 7.12 (t, J = 7.6 Hz, 2H), 7.42 (s, 1H), 7.60 (m, 4H), 7.95 (s, 1H). ^{13}C NMR (100 MHz, DMSO-d_6): δ 111.6, 114.0, 116.6, 126.0, 128.7, 128.9, 129.6, 132.2, 134.1, 136.6, 144.9, 147.9 ppm.

6.3.4. (*Z*)-5-Amino-1-(3-chlorophenyl)-*N*′-phenyl-1*H*-imidazole-4-carbohydrazonamide (1c). 5-Amino-1-(3-chlorophenyl)-1*H*-imidazole-4-carbimidoyl cyanide (1.00 g, 4.1 mmol), ethanol (3 mL), phenylhydrazine (0.602 mL, 6.2 mmol) and acetic acid (10 μL). After 24 hours at 8 °C, compound **1c** was obtained pure (1.04 g, 3.2 mmol, 78%). M.p. > 161 °C (dec.). ^1H NMR (400 MHz, DMSO-d_6): δ 5.77 (brs, 2H), 5.81 (brs, 2H), 6.58 (t, J = 7.2 Hz, 1H), 6.84 (d, J = 8.4 Hz, 2H), 7.12 (t, J = 8.0 Hz, 2H), 7.47 (s, 1H), 7.52 (t, J = 7.2 Hz, 1H), 7.59 (d, J = 8.0 Hz,

1H), 7.56 (d, J = 8.0 Hz, 1H), 7.70 (t, J = 2.0 Hz, 1H), 7.96 (s, 1H). ^{13}C NMR (100 MHz, DMSO-d_6): δ 111.6, 114.1, 116.6, 122.7, 123.9, 127.6, 128.7, 129.0, 131.3, 133.9, 136.5, 136.5, 144.7, 147.8 ppm.

6.3.5. (*Z*)-5-Amino-1-(4-bromophenyl)-*N*′-phenyl-1*H*-imidazole-4-carbohydrazonamide (1d). 5-Amino-1-(4-bromophenyl)-1*H*-imidazole-4-carbimidoyl cyanide (1.00 g, 3.5 mmol), ethanol (4 mL), phenylhydrazine (0.509 mL, 5.3 mmol) and acetic acid (10 μL). After 4 hours at 8 °C, compound **1d** was obtained pure (0.896 g, 2.4 mmol, 70%). M.p. > 175 °C (dec.). ^{1}H NMR (400 MHz, DMSO-d_6): δ 5.72 (brs, 2H), 5.80 (brs, 2H), 6.58 (t, J = 6.9 Hz, 1H), 6.85 (d, J = 7.2 Hz, 2H), 7.12 (t, J = 8.4 Hz, 2H), 7.42 (s, 1H), 7.52 (d, J = 8.8 Hz, 2H), 7.75 (d, J = 8.4 Hz, 2H), 7.95 (s, 1H). ^{13}C NMR (100 MHz, DMSO-d_6): δ 111.6, 114.0, 116.6, 120.6, 126.3, 128.8, 128.8, 132.6, 134.5, 136.6, 144.9, 147.9 ppm.

6.3.6. (*Z*)-5-Amino-1-(3-bromophenyl)-*N*′-phenyl-1*H*-imidazole-4-carbohydrazonamide (1e). 5-Amino-1-(3-bromophenyl)-1*H*-imidazole-4-carbimidoyl cyanide (0.506 g, 1.7 mmol), ethanol (2 mL), phenylhydrazine (0.255 mL, 2.6 mmol) and acetic acid (5 μL) After 5:30 hours at 8 °C, compound **1e** was obtained pure (0.477 g, 1.3 mmol, 76%). M.p. > 162 °C (dec.). ^{1}H NMR (400 MHz, DMSO-d_6): δ 5.76 (brs, 2H), 5.80 (brs, 2H), 6.58 (t, J = 7.2 Hz, 1H), 6.84 (d, J = 8.8 Hz, 2H), 7.12 (t, J = 7.8 Hz, 2H), 7.47 (s, 1H), 7.51 (t, J = 8.0 Hz, 1H), 7.59 (dd, J = 8.8 Hz, J = 2.0 Hz, 1H), 7.65 (dd, J = 8.8 Hz, J = 2.0 Hz, 1H), 7.82 (t, J = 2.0 Hz, 1H), 7.96 (s, 1H). ^{13}C NMR (100 MHz, DMSO-d_6): δ 111.6, 114.1, 116.6, 122.2, 123.1, 126.7, 128.8, 129.0, 130.5, 131.5, 136.5, 136.7, 144.7, 147.8 ppm.

6.3.7. (*Z*)-5-Amino-*N*′-phenyl-1-(*p*-tolyl)-1*H*-imidazole-4-carbohydrazonamide (1f). 5-Amino-1-(*p*-tolyl)-1*H*-imidazole-4-carbimidoyl cyanide (0.500 g, 2.2 mmol), ethanol (2 mL), phenylhydrazine (0.322 mL, 3.3 mmol) and acetic acid (5 μL). After 7:30 hours at 8 °C, compound **1f** was obtained pure (0.558 g, 1.8 mmol, 83%). M.p. > 163 °C (dec.). ^{1}H NMR (400 MHz, DMSO-d_6): δ 2.37 (s, 3H), 5.63 (brs, 2H), 5.78 (brs, 2H), 6.58 (t, J = 7.2 Hz, 1H), 6.84 (d, J = 8.4 Hz, 2H), 7.12 (t, J = 7.8 Hz, 2H), 7.35 (s, 1H), 7.35 (d, J = 8.8 Hz, 2H), 7.42 (d, J = 8.4 Hz, 2H), 7.93 (s, 1H). ^{13}C NMR (100 MHz, DMSO-d_6): δ 20.6, 111.6, 113.7, 116.6, 124.1, 128.7, 128.9, 130.1, 132.6, 136.7, 137.3, 145.1, 147.9 ppm.

6.3.8. (*Z*)-5-Amino-1-(4-methoxyphenyl)-*N*′-phenyl-1*H*-imidazole-4-carbohydrazonamide (1g). 5-Amino-1-(4-methoxyphenyl)-1*H*-imidazole-4-carbimidoyl cyanide (1.00 g, 4.2 mmol), ethanol (3 mL), phenylhydrazine (0.692 mL, 6.3 mmol) and acetic acid (10 μL). After 26 hours at 8 °C, compound **1g** was obtained pure by filtration with cold ethanol and diethyl ether (0.944 g, 2.9 mmol, 71%). M.p. > 189 °C (dec.). ^{1}H NMR (400 MHz, DMSO-d_6): δ 3.81 (s, 3H), 5.57 (brs, 2H), 5.78 (brs, 2H), 6.57 (t, J = 7.2 Hz, 1H), 6.84 (d, J = 7.6 Hz, 2H), 7.09 (d, J = 9.2 Hz, 2H), 7.12 (t, J = 7.2 Hz, 2H), 7.31 (s, 1H), 7.44 (d, J = 8.8 Hz, 2H), 7.92 (s, 1H). ^{13}C NMR (100 MHz, DMSO-d_6): δ 55.5, 111.6, 113.5, 114.8, 116.6, 125.9, 127.9, 128.7, 129.0, 136.9, 145.2, 147.9, 158.7 ppm.

6.3.9. (*Z*)-5-Amino-*N*′,1-diphenyl-1*H*-imidazole-4-carbohydrazonamide (1h). 5-Amino-1-phenyl-1*H*-imidazole-4-carbimidoyl cyanide (1.00 g, 4.7 mmol), ethanol (3 mL), phenylhydrazine (0.700 mL, 7.1 mmol) and acetic acid (10 μL). After 26 hours at 8 °C, compound **1h** was obtained pure (1.27 g, 3.2 mmol, 68%). M.p. > 155 °C (dec.). ^{1}H NMR (400 MHz, DMSO-d_6): δ 5.68 (brs, 2H), 5.80 (brs, 2H), 6.58 (t, J = 7.2 Hz, 1H), 6.84 (d, J = 8.4 Hz, 2H), 7.12 (t, J = 8.0 Hz, 2H), 7.41 (s, 1H), 7.46 (m, 1H), 7.56 (m, 4H), 7.95 (s, 1H). ^{13}C NMR (100 MHz, DMSO-d_6): δ 111.6, 113.8, 116.6, 124.1, 127.7, 128.7, 128.9, 129.7, 135.2, 136.7, 145.0, 147.9 ppm.

6.3.10. General procedure for the synthesis of azoimidazoles 4. The general procedure to obtain azoimidazoles **4** consisted in the reaction between amidrazones **1** and piperidine. To a suspension of the corresponding amidrazone **1** (0.31–0.33 mmol) in acetonitrile (2 mL) and water (1 mL), piperidine (2 molar equivalents) was added under magnetic stirring in an ice bath. Once a homogenous mixture was obtained, potassium iodide (0.2 molar equivalents) was added. The suspensions were stirred at 0 °C for 3:30 h until the reactions were completed according to a TLC in DCM/EtOH (9 : 1), presenting R_f values ranging from 0.49 to 0.84. At this point, a filtration was performed with water, acetonitrile and diethyl ether and the pure azoimidazoles **4** were obtained.

6.3.11. (*Z*)-5-Amino-1-(4-chlorophenyl)-*N*′-phenyl-2-(piperidin-1-yl)-1*H*-imidazole-4-carbohydrazonamide (4d_II). Compound **1b** (0.100 g; 0.31 mmol), acetonitrile, water, piperidine (61 μL; 0.62 mmol), potassium iodide (11 mg; 0.06 mmol). After 3:30 h at 0 °C, compound **4d_II** was obtained pure (0.085 g, 0.21 mmol, 67%) and later evolver into tautomer **4d_I** in the NMR tube. (**4d_II**): ^{1}H NMR (400 MHz, DMSO-d_6): δ 1.37 (m, 6H), 2.55 (m, 4H), 6.09 (brs, 2H), 6.39 (s, 1H), 6.77 (t, J = 7.2 Hz, 1H), 7.01 (d, J = 7.6 Hz, 2H), 7.25 (t, J = 7.6 Hz, 2H), 7.39 (d, J = 8.8 Hz, 2H), 7.98 (d, J = 9.2 Hz, 2H), 9.11 (s, 1H), 9.36 (s, 1H) ppm. ^{13}C NMR (100 MHz, DMSO-d_6): δ 45.9, 95.2, 112.0, 119.8, 121.8, 127.7, 129.2 ppm. (**4d_I**): ^{1}H NMR (400 MHz, DMSO-d_6): δ 1.38 (m, 6H), 2.77 (m, 4H), 5.32 (brs, 2H), 5.62 (brs, 2H), 6.55 (t, J = 7.2 Hz, 1H), 6.80 (d, J = 7.2 Hz, 2H), 7.09 (t, J = 7.2 Hz, 2H), 7.49 (d, J = 8.8 Hz, 2H), 7.61 (d, J = 8.8 Hz, 2H), 7.86 (s, 1H) ppm. ^{13}C NMR (100 MHz, DMSO-d_6): δ 23.6, 25.0, 50.6, 108.5, 111.6, 116.4, 128.5, 128.7, 129.4, 132.3, 133.9, 135.2, 144.7, 145.7, 148.0 ppm.

6.3.12. (*Z*)-5-Amino-1-(3-chlorophenyl)-*N*′-phenyl-2-(piperidin-1-yl)-1*H*-imidazole-4 carbohydrazonamide (4f_II). Compound **1c** (0.100 g; 0.31 mmol), acetonitrile, water, piperidine (61 μL; 0.62 mmol), potassium iodide (11 mg; 0.06 mmol). After 3:30 h at 0 °C, compound **4f_II** was obtained pure (0.094 g, 0.23 mmol, 74%) and later evolved into tautomer **4d_I** in the NMR tube. (**4f_II**): ^{1}H NMR (400 MHz, DMSO-d_6): δ 1.37 (m, 6H), 2.56 (m, 4H), 6.10 (brs, 2H), 6.42 (s, 1H), 6.78 (t, J = 7.2 Hz, 1H), 7.02 (d, J = 7.6 Hz, 2H), 7.10 (dd, J = 8.0 Hz, J = 2 Hz, 1H), 7.26 (t, J = 7.2 Hz, 2H), 7.37 (t, J = 8.2 Hz, 1H), 7.80 (dd, J = 8.4 Hz, J = 2 Hz, 1H), 8.27 (t, J = 2 Hz, 1H), 9.12 (s, 1H), 9.37 (s, 1H) ppm. (**4f_I**): ^{1}H NMR (400 MHz, DMSO-d_6): δ 1.37 (m, 6H), 2.78 (m, 4H), 5.37 (brs, 2H), 5.63 (brs, 2H), 6.55 (t, J = 7.2 Hz, 1H), 6.82 (d, J = 7.6 Hz, 2H), 7.10 (t, J = 7.6 Hz, 2H), 7.48 (dd, J = 7.8 Hz, J = 2 Hz, 1H), 7.52 (dd, J = 8.2 Hz, J = 2 Hz, 1H), 7.59 (t, J = 2 Hz, 1H), 7.59 (t, J = 7.8 Hz, 1H), 7.87 (s, 1H) ppm.

^{13}C NMR (100 MHz, DMSO-d_6): δ 23.6, 25.0, 50.6, 108.7, 111.6, 116.4, 125.4, 126.5, 127.9, 128.7, 131.0, 133.4, 135.1, 136.4, 144.6, 145.6, 148.0 ppm.

6.3.13. (*Z*)-5-Amino-*N*′-phenyl-2-(piperidin-1-yl)-1-(*p*-tolyl)-1*H*-imidazole-4-carbohydrazonamide (4j_I). Compound **1f** (0.100 g; 0.33 mmol), acetonitrile, water, piperidine (61 μL; 0.66 mmol), potassium iodide (11 mg; 0.07 mmol). After 3:30 h at 0 °C, compound **4j_I** was obtained pure (0.086 g, 0.22 mmol, 67%). ^{1}H NMR (400 MHz, DMSO-d_6): δ 1.37 (m, 6H), 2.37 (s, 3H), 2.78 (m, 4H), 5.21 (brs, 2H), 5.60 (brs, 2H), 6.54 (t, J = 7.2 Hz, 1H), 6.80 (d, J = 7.6 Hz, 2H), 7.08 (t, J = 7.4 Hz, 2H), 7.32 (d, J = 8.8 Hz, 2H), 7.34 (d, J = 8.8 Hz, 2H), 7.84 (s, 1H) ppm. ^{13}C NMR (100 MHz, DMSO-d_6): δ 20.7, 23.7, 25.0, 50.5, 108.1, 111.6, 116.4, 126.4, 128.7, 129.9, 132.4, 135.4, 137.3, 144.9, 145.9, 148.1 ppm.

6.3.14. General procedure for the synthesis of azoimidazoles 5. The general procedure to obtain azoimidazoles **5** consisted in the reaction between 5-aminoimidazole-4-carboxamidrazones and a secondary amine (piperidine, dimethylamine or pyrrolidine). To a suspension of the corresponding amidrazone **1** (0.27–0.34 mmol) in acetonitrile (2 mL) and water (1 mL), triethylamine (3 molar equivalents) and the desired amine (2 molar equivalents) were added under magnetic stirring. Once a homogenous mixture was obtained, potassium iodide (0.2 molar equivalents) was added. The suspensions were stirred at 40 °C for 4–5 h until the reactions were completed according to a TLC in DCM/EtOH (7 : 3), presenting R_f values ranging from 0.62 to 0.88. At this point a filtration was performed with water, acetonitrile and diethyl ether and the pure azoimidazoles **5** were obtained.

6.3.15. (4*E*)-4-(Amino(phenyldiazenyl)methylene)-*N*-(4-fluorophenyl)-2-(piperidin-1-yl)-4*H*-imidazol-5-amine (5a). Compound **1a** (0.100 g, 0.32 mmol), acetonitrile, water, triethylamine (135 μL, 0.96 mmol), piperidine (64 μL, 0.64 mmol), potassium iodide (0.011 g, 0.06 mmol). After 4 hours at 40 °C, compound **5a** was obtained pure (0.098 g; 0.25 mmol; 79%). M.p. > 191 °C (dec.). ^{1}H NMR (400 MHz, DMSO-d_6): δ 1.65 (m, 6H), 3.88 (s, 4H), 5.86 (brs, 2H), 7.25 (t, J = 9.0 Hz, 2H), 7.42 (t, J = 7.4 Hz, 1H), 7.58 (t, J = 8.0 Hz, 2H), 7.69 (d, J = 7.6 Hz, 2H), 7.82 (dd, J = 9.2 Hz, J = 4.7 Hz, 2H), 10.02 (s, 1H) ppm. ^{13}C NMR (100 MHz, DMSO-d_6): δ 22.5, 23.8, 25.8, 46.3, 115.9 (J = 23 Hz), 119.9 (J = 8 Hz), 121.7, 129.4, 129.7, 135.4 (J = 3 Hz), 136.9, 146.4, 152.9, 157.9 (J = 239 Hz), 164.6, 170.3 ppm. IR: ν 3452w, 3326m, 2934m, 2856w, 1944w, 1607s, 1586m, 1568m, 1549w, 1533s, 1507s cm^{-1}. Analysis calc. ($C_{21}H_{22}FN_7$·0.1H_2O): C 64.14 N 24.93 H 5.69; found: C 64.40 N 24.67 H 5.92.

6.3.16. (4*E*)-4-(Amino(phenyldiazenyl)methylene)-*N*5-(4-fluorophenyl)-N^2,N^2-dimethyl-4*H*-imidazole-2,5-diamine (5b). Compound **1a** (0.100 g, 0.32 mmol), acetonitrile, water, triethylamine (135 μL, 0.96 mmol), dimethylamine (82 μL, 0.64 mmol), potassium iodide (0.011 g, 0.06 mmol). After 4 hours at 40 °C, compound **5b** was obtained pure (0.048 g; 0.14 mmol; 42%). M.p. > 198 °C (dec.). ^{1}H NMR (400 MHz, DMSO-d_6): δ 3.32 (s, 6H), 5.77 (brs, 2H), 7.22 (t, J = 8.8 Hz, 2H), 7.43 (t, J = 7.2 Hz, 1H), 7.58 (t, J = 7.8 Hz, 2H), 7.70 (d, J = 7.6 Hz, 2H), 7.83 (q, J = 4.7 Hz, 2H), 9.97 (s, 1H) ppm. ^{13}C NMR (100 MHz, DMSO-d_6): δ 37.5, 115.6 (J = 22 Hz), 119.8 (J = 8 Hz), 121.5, 129.2, 129.4, 135.3 (J = 2 Hz), 136.9, 146.2, 152.8, 157.8 (J = 239 Hz), 164.4, 171.5 ppm. IR: ν 3336m, 2927w, 2878w, 2800w, 1618s, 1599m, 1567m, 1538m, 1506s cm^{-1}. Analysis calc. ($C_{18}H_{18}FN_7$·0.3Et_2O·0.1KI): C 59.10 N 25.13 H 5.42; found: C 59.26 N 25.05 H 5.41.

6.3.17. (4*E*)-4-(Amino(phenyldiazenyl)methylene)-*N*-(4-fluorophenyl)-2-(pyrrolidin-1-yl)-4*H*-imidazol-5-amine (5c). Compound **1a** (0.100 g, 0.32 mmol), acetonitrile, water, triethylamine (135 μL, 0.96 mmol), pyrrolidine (54 μL, 0.64 mmol), potassium iodide (0.011 g, 0.06 mmol). After 4 hours at 40 °C, compound **5c** was obtained pure (0.084 g; 0.22 mmol; 70%). M.p. > 214 °C (dec.). ^{1}H NMR (400 MHz, DMSO-d_6): δ 1.96 (m, 4H), 3.72 (m, 4H), 5.83 (s, 2H), 7.23 (t, J = 8.8 Hz, 2H), 7.42 (t, J = 7.4 Hz, 1H), 7.58 (t, J = 7.8 Hz, 2H), 7.70 (d, J = 7.6 Hz, 2H), 7.84 (q, J = 4.5 Hz, 2H), 10.02 (s, 1H) ppm. ^{13}C NMR (100 MHz, DMSO-d_6): δ 24.6, 47.5, 115.5 (J = 23 Hz), 119.8 (J = 8 Hz), 129.2, 129.4, 135.3, 136.9, 146.3, 152.8, 157.8 (J = 238 Hz), 164.3, 169.0 ppm. IR: ν 3454w, 3336m, 2916w, 2875w, 1622w, 1610m, 1590s, 1564w, 1558m, 1535s cm^{-1}. Analysis calc. ($C_{20}H_{20}FN_7$·0.5H_2O·0.4Et_2O): C 62.35 N 23.56 H 6.06; found: C 62.21 N 23.82 H 6.32.

6.3.18. (4*E*)-4-(Amino(phenyldiazenyl)methylene)-*N*-(4-chlorophenyl)-2-(piperidin-1-yl)-4*H*-imidazol-5-amine (5d). Compound **1b** (0.100 g, 0.31 mmol), acetonitrile, water, triethylamine (128 μL, 0.93 mmol), piperidine (61 μL, 0.62 mmol), potassium iodide (0.011 g, 0.06 mmol). After 4 hours at 40 °C, compound **5d** was obtained pure (0.109 g; 0.27 mmol; 87%). M.p. > 211 °C (dec.). ^{1}H NMR (400 MHz, DMSO-d_6): δ 1.64 (m, 6H), 3.89 (s, 4H), 5.91 (brs, 2H), 7.42 (t, J = 7.2 Hz, 1H), 7.43 (d, J = 8.8 Hz, 2H), 7.58 (t, J = 7.8 Hz, 2H), 7.70 (d, J = 7.6 Hz, 2H), 7.80 (d, J = 8.8 Hz, 2H), 10.06 (s, 1H) ppm. ^{13}C NMR (100 MHz, DMSO-d_6): δ 23.6, 25.5, 46.2, 119.7, 121.5, 126.5, 128.9, 129.3, 129.4, 136.6, 137.6, 146.3, 152.8, 164.4, 170.0 ppm. IR: ν 3450w, 3333m, 2945w, 2928w, 1611s, 1582s, 1536s cm^{-1}. Analysis calc. ($C_{21}H_{22}ClN_7$): C 61.84 N 24.04 H 5.44; found: C 61.91 N 23.99 H 5.33.

6.3.19. (4*E*)-4-(Amino(phenyldiazenyl)methylene)-*N*5-(4-chlorophenyl)-N^2,N^2-dimethyl-4*H*-imidazole-2,5-diamine (5e). Compound **1b** (0.100 g, 0.31 mmol), acetonitrile, water, triethylamine (128 μL, 0.93 mmol), dimethylamine (103 μL, 0.62 mmol), potassium iodide (0.011 g, 0.06 mmol). After 4 hours at 40 °C, compound **5e** was obtained (0.093 g; 0.25 mmol; 82%). M.p. > 203 °C (dec.). ^{1}H NMR (400 MHz, DMSO-d_6): δ 3.32 (s, 6H), 5.81 (brs, 2H), 7.42 (d, J = 8.8 Hz, 2H), 7.44 (t, J = 6.8 Hz, 1H), 7.58 (t, J = 8.0 Hz, 2H), 7.70 (d, J = 8.0 Hz, 2H), 7.81 (d, J = 8.8 Hz, 2H), 10.00 (s, 1H) ppm. ^{13}C NMR (100 MHz, DMSO-d_6): δ 37.5, 119.7, 121.6, 126.5, 128.8, 129.3, 129.4, 136.7, 137.6, 146.3, 152.8, 164.3, 171.2 ppm. IR: ν 3448w, 3334m, 3061w, 2916w, 1614s, 1586s, 1550w, 1539s cm^{-1}. Analysis calc. ($C_{18}H_{18}ClN_7$·0.9H_2O·0.3Et_2O): C 56.76 N 24.13 H 5.66; found: C 56.87 N 24.13 H 5.65.

6.3.20. (4*E*)-4-(Amino(phenyldiazenyl)methylene)-*N*-(3-chlorophenyl)-2-(piperidin-1-yl)-4*H*-imidazol-5-amine (5f). Compound **1c** (0.100 g, 0.31 mmol), acetonitrile, water, triethylamine (128 μL, 0.93 mmol), piperidine (61 μL,

0.62 mmol), potassium iodide (0.011 g, 0.06 mmol). After 4 hours at 40 °C, compound **5f** was obtained pure (0.099 g; 0.24 mmol; 79%). M.p. > 190 °C (dec.). ^{1}H NMR (400 MHz, DMSO-d_6): δ 1.66 (m, 6H), 3.89 (s, 4H), 5.96 (brs, 2H), 7.12 (dd, J = 9.2 Hz, J = 2.0 Hz, 1H), 7.42 (t, J = 8.0 Hz, 1H), 7.45 (t, J = 7.2 Hz, 1H), 7.57 (d, J = 9.2 Hz, 1H), 7.58 (t, J = 7.8 Hz, 2H), 7.72 (d, J = 8.4 Hz, 2H), 8.03 (t, J = 2.2 Hz, 1H), 10.10 (s, 1H) ppm. ^{13}C NMR (100 MHz, DMSO-d_6): δ 23.8, 25.7, 46.4, 116.8, 117.8, 121.9, 122.6, 129.6, 129.6, 130.9, 133.4, 136.5, 140.2, 146.6, 152.9, 164.5, 169.9 ppm. IR: ν 3483w, 3373m, 2934m, 2921w, 2855w, 1615s, 1595m, 1577s, 1520s cm^{-1}. Analysis calc. ($C_{21}H_{22}ClN_7$): C 61.84 N 24.04 H 5.44; found: C 61.82 N 23.81 H 5.67.

6.3.21. (4*E*)-4-(Amino(phenyldiazenyl)methylene)-*N*-(4-bromophenyl)-2-(piperidin-1-yl)-4*H*-imidazol-5-amine (5g). Compound **1d** (0.100 g, 0.27 mmol), acetonitrile, water, triethylamine (112 μL, 0.81 mmol), piperidine (54 μL, 0.54 mmol), potassium iodide (0.010 g, 0.05 mmol). After 4 hours at 40 °C, compound **5g** was obtained (0.101 g; 0.22 mmol; 82%). M.p. > 211 °C (dec.). ^{1}H NMR (400 MHz, DMSO-d_6): δ 1.66 (m, 6H), 3.89 (s, 4H), 5.92 (brs, 2H), 7.44 (t, J = 7.4 Hz, 1H), 7.57 (d, J = 8.8 Hz, 2H), 7.59 (t, J = 7.8 Hz, 2H), 7.70 (d, J = 7.6 Hz, 2H), 7.75 (d, J = 9.2 Hz, 2H), 10.06 (s, 1H) ppm. ^{13}C NMR (100 MHz, DMSO-d_6): δ 23.8, 25.7, 46.5, 114.6, 120.3, 121.8, 129.6, 129.7, 132.0, 136.7, 138.2, 146.5, 152.9, 164.5, 170.0 ppm. IR: ν 3487w, 3371m, 1928w, 2927w, 2848w, 1889w, 1614s, 1590w, 1581m, 1558s, 1544s, 1525s, cm^{-1}. Analysis calc. ($C_{21}H_{22}BrN_7{\cdot}0.3H_2O$): C 55.10 N 21.42 H 4.98; found: C 55.28 N 21.15 H 5.23.

6.3.22. (4*E*)-4-(Amino(phenyldiazenyl)methylene)-*N*5-(4-bromophenyl)-N^2,N^2-dimethyl-4*H*-imidazole-2,5-diamine (5h). Compound **1d** (0.100 g, 0.27 mmol), acetonitrile, water, triethylamine (112 μL, 0.81 mmol), dimethylamine (68 μL, 0.54 mmol), potassium iodide (0.010 g, 0.05 mmol). After 4 hours at 40 °C, compound **5h** was obtained pure (0.095 g; 0.23 mmol; 86%). M.p. > 205 °C (dec.). ^{1}H NMR (400 MHz, DMSO-d_6): δ 3.32 (s, 6H), 5.82 (brs, 2H), 7.44 (t, J = 7.2 Hz, 1H), 7.56 (d, J = 8.8 Hz, 2H), 7.58 (t, J = 7.6 Hz, 2H), 7.70 (d, J = 7.6 Hz, 2H), 7.76 (d, J = 9.2 Hz, 2H), 10.00 (s, 1H) ppm. ^{13}C NMR (100 MHz, DMSO-d_6): δ 37.5, 114.4, 120.1, 121.6, 129.4, 129.4, 131.7, 136.7, 138.0, 146.3, 152.8, 164.3, 171.2 ppm. IR: ν 3338m, 3074w, 2921w, 2875w, 2802w, 1615s, 1586s, 1548m, 1538s cm^{-1}. Analysis calc. ($C_{18}H_{18}BrN_7{\cdot}1.5H_2O{\cdot}0.2Et_2O$): C 49.72 N 21.59 H 5.11; found: C 49.68 N 21.62 H 4.80.

6.3.23. (4*E*)-4-(Amino(phenyldiazenyl)methylene)-*N*-(3-bromophenyl)-2-(piperidin-1-yl)-4*H*-imidazol-5-amine (5i). Compound **1e** (0.100 g, 0.27 mmol), acetonitrile, water, triethylamine (112 μL, 0.81 mmol), piperidine (54 μL, 0.54 mmol), potassium iodide (0.010 g, 0.05 mmol). After 4 hours at 40 °C, compound **5i** was obtained pure (0.117 g; 0.26 mmol; 94%). M.p. > 176 °C (dec.). ^{1}H NMR (400 MHz, DMSO-d_6): 1.66 (m, 6H), 3.88 (s, 4H), 5.95 (brs, 2H), 7.24 (d, J = 8.8 Hz, 1H), 7.35 (t, J = 8.0 Hz, 1H), 7.45 (t, J = 7.2 Hz, 1H), 7.58 (t, J = 7.8 Hz, 2H), 7.63 (d, J = 9.2 Hz, 1H), 7.71 (d, J = 7.6 Hz, 2H), 8.15 (t, J = 2.0 Hz, 1H), 10.10 (s, 1H) ppm. ^{13}C NMR (100 MHz, DMSO-d_6): δ 23.8, 25.7, 46.5, 117.1, 120.7, 121.9, 121.9, 125.4, 129.6, 129.7, 131.2, 136.5, 140.3, 146.6, 153.0, 164.5, 169.9 ppm. IR: ν 3386w, 2937m, 2856w, 1610s, 1592m, 1576m, 1563w, 1531s cm^{-1}. Analysis calc. ($C_{21}H_{22}BrN_7{\cdot}1.3H_2O$): C 53.01 N 20.61 H 5.21; found: C 53.14 N 20.27 H 4.91.

6.3.24. (4*E*)-4-(Amino(phenyldiazenyl)methylene)-2-(piperidin-1-yl)-*N*-(*p*-tolyl)-4*H*-imidazol-5-amine (5j). Compound **1f** (0.100 g, 0.33 mmol), acetonitrile, water, triethylamine (136 μL, 0.99 mmol), piperidine (71 μL, 0.66 mmol), potassium iodide (0.011 g, 0.07 mmol). After 4 hours at 40 °C, compound **5j** was obtained (0.104 g; 0.27 mmol; 81%). M.p. > 184 °C (dec.). ^{1}H NMR (400 MHz, DMSO-d_6): δ 1.65 (m, 6H), 2.28 (s, 3H), 3.88 (s, 4H), 5.82 (brs, 2H), 7.20 (d, J = 8.4 Hz, 2H), 7.42 (t, J = 7.4 Hz, 1H), 7.58 (t, J = 7.8 Hz, 2H), 7.68 (m, 4H), 10.02 (s, 1H) ppm. ^{13}C NMR (100 MHz, DMSO-d_6): δ 20.5, 23.8, 25.8, 46.4, 118.2, 121.6, 129.3, 129.6, 129.7, 132.3, 136.4, 137.4, 146.3, 153.0, 164.6, 170.6 ppm. IR: ν 3347m, 2936m, 2918w, 2854w, 1604s, 1585m, 1564w, 1538m, 1532s, 1513m cm^{-1}. Analysis calc. ($C_{22}H_{25}N_7{\cdot}0.3H_2O$): C 67.26 N 24.96 H 6.57; found: C 67.59 N 24.86 H 6.89.

6.3.25. (4*E*)-4-(Amino(phenyldiazenyl)methylene)-N^2,N^2-dimethyl-*N*5-(*p*-tolyl)-4*H*-imidazole-2,5-diamine (5k). Compound **1f** (0.100 g, 0.33 mmol), acetonitrile, water, triethylamine (136 μL, 0.99 mmol), dimethylamine (83 μL, 0.66 mmol), potassium iodide (0.011 g, 0.07 mmol). After 4 hours at 40 °C, compound **5k** was obtained pure (0.074 g; 0.21 mmol; 61%). M.p. > 205 °C (dec.). ^{1}H NMR (400 MHz, DMSO-d_6): δ 2.29 (s, 3H), 3.32 (s, 6H), 5.72 (brs, 2H), 7.20 (d, J = 8.0 Hz, 2H), 7.42 (t, J = 7.4 Hz, 1H), 7.57 (t, J = 7.8 Hz, 2H), 7.68 (d, J = 8.4 Hz, 2H), 7.68 (d, J = 8.4 Hz, 2H), 9.96 (s, 1H) ppm. ^{13}C NMR (100 MHz, DMSO-d_6): δ 20.2, 37.5, 118.1, 121.4, 129.1, 129.4, 129.4, 132.2, 137.3, 137.4, 146.1, 152.9, 164.4, 171.8 ppm. IR: ν 3454w, 3336m, 2915w, 2875w, 1622w, 1610m, 1590s, 1564w, 1558w, 1535s cm^{-1}. Analysis calc. ($C_{19}H_{21}N_7{\cdot}0.5H_2O{\cdot}0.4Et_2O$): C 59.10 N 25.13 H 5.42; found: C 59.25 N 25.05 H 5.41.

6.3.26. (4*E*)-4-(Amino(phenyldiazenyl)methylene)-2-(pyrrolidin-1-yl)-*N*-(*p*-tolyl)-4*H*-imidazol-5-amine (5l). Compound **1f** (0.100 g, 0.33 mmol), acetonitrile, water, triethylamine (136 μL, 0.99 mmol), pyrrolidine (54 μL, 0.66 mmol), potassium iodide (0.011 g, 0.07 mmol). After 4 hours at 40 °C, compound **5l** was obtained pure (0.080 g; 0.22 mmol; 66%). M.p. > 213 °C (dec.). ^{1}H NMR (400 MHz, DMSO-d_6): δ 1.97 (s, 4H), 2.29 (s, 3H), 3.74 (m, 4H), 5.70 (brs, 2H), 7.20 (d, J = 8.4 Hz, 2H), 7.41 (t, J = 7.2 Hz, 1H), 7.57 (t, J = 8.0 Hz, 2H), 7.70 (d, J = 7.6 Hz, 2H), 7.71 (d, J = 8.8 Hz, 2H), 9.99 (s, 1H) ppm. ^{13}C NMR (100 MHz, DMSO-d_6): δ 20.2, 24.6, 47.6, 118.1, 121.4, 129.0, 129.4, 129.4, 132.1, 136.3, 137.4, 146.2, 152.9, 164.3, 169.3 ppm. IR: ν 3461w, 3340m, 1968w, 2949w, 2873w, 1606s, 1584s, 1562m, 1531s, 1511m cm^{-1}. Analysis calc. ($C_{21}H_{23}N_7{\cdot}0.5H_2O{\cdot}0.4Et_2O$): C 65.87 N 23.79 H 6.85; found: C 65.85 N 23.82 H 6.90.

6.3.27. (4*E*)-4-(Amino(phenyldiazenyl)methylene)-*N*-(4-methoxyphenyl)-2-(piperidin-1-yl)-4*H*-imidazol-5-amine (5m). Compound **1g** (0.100 g, 0.31 mmol), acetonitrile, water, triethylamine (130 μL, 0.93 mmol), piperidine (61 μL,

0.62 mmol), potassium iodide (0.011 g, 0.06 mmol). After 4 hours at 40 °C, compound **5m** was obtained pure (0.084 g; 0.21 mmol; 67%). M.p. > 180 °C (dec.). ^{1}H NMR (400 MHz, DMSO-d_6): δ 1.64 (m, 6H), 3.75 (s, 3H), 3.88 (s, 4H), 5.92 (brs, 2H), 6.99 (d, J = 8.8 Hz, 2H), 7.40 (t, J = 7.2 Hz, 1H), 7.57 (t, J = 7.8 Hz, 2H), 7.67 (d, J = 7.6 Hz, 2H), 7.73 (d, J = 9.2 Hz, 2H), 9.98 (s, 1H) ppm. ^{13}C NMR (100 MHz, DMSO-d_6): δ 22.5, 23.8, 25.8, 46.3, 55.3, 114.5, 119.6, 121.6, 129.4, 129.6, 132.3, 137.5, 146.2, 153.0, 155.3, 164.4, 170.8 ppm. IR: ν 3336m, 2940w, 2859w, 1612s, 1591m, 1568s, 1538s, 1506s cm^{-1}. Analysis calc. ($C_{22}H_{25}N_7O{\cdot}0.5H_2O{\cdot}0.9Et_2O{\cdot}2CH_3CN$): C 63.54 N 22.53 H 7.35; found: C 63.59 N 22.86 H 7.67.

6.3.28. (4*E*)-4-(Amino(phenyldiazenyl)methylene)-*N*5-(4-methoxyphenyl)-N^2,N^2-dimethyl-4*H*-imidazole-2,5-diamine (5n). Compound **1g** (0.100 g, 0.31 mmol), acetonitrile, water, triethylamine (130 μL, 0.93 mmol), dimethylamine (79 μL, 0.62 mmol), potassium iodide (0.011 g, 0.06 mmol). After 4 hours at 40 °C, compound **5n** was obtained (0.084 g; 0.21 mmol; 67%). M.p. > 210 °C (dec.). ^{1}H NMR (400 MHz, DMSO-d_6): δ 3.32 (s, 6H), 3.76 (s, 3H), 5.68 (brs, 2H), 6.99 (d, J = 8.8 Hz, 2H), 7.41 (t, J = 7.4 Hz, 1H), 7.57 (t, J = 7.8 Hz, 2H), 7.68 (d, J = 7.6 Hz, 2H), 7.74 (d, J = 9.2 Hz, 2H), 9.93 (s, 1H) ppm. ^{13}C NMR (100 MHz, DMSO-d_6): δ 37.5, 55.2, 114.4, 119.5, 121.4, 128.9, 129.4, 132.2, 137.5, 146.0, 152.9, 155.3, 164.3, 171.9 ppm. IR: ν 3438m, 3328m, 2910w, 2832m, 1868m, 1622m, 1592s, 1567m, 1558m, 1533m, 1506m cm^{-1}. Analysis calc. ($C_{19}H_{21}N_7O{\cdot}0.2Et_2O{\cdot}0.2CH_3CN$): C 62.78 N 26.10 H 6.16; found: C 62.87 N 26.17 H 6.24.

6.3.29. (4*E*)-4-(Amino(phenyldiazenyl)methylene)-*N*-(4-methoxyphenyl)-2-(pyrrolidin-1-yl)-4*H*-imidazol-5-amine (5o). Compound **1g** (0.100 g, 0.31 mmol) in acetonitrile, water, triethylamine (130 μL, 0.93 mmol), pyrrolidine (52 μL, 0.62 mmol), potassium iodide (0.011 g, 0.06 mmol). After 4 hours at 40 °C, compound **5o** was obtained pure (0.082 g; 0.21 mmol; 68%). M.p. > 223 °C (dec.). ^{1}H NMR (400 MHz, DMSO-d_6): δ 1.97 (s, 4H), 3.74 (m, 4H), 3.76 (s, 3H), 5.67 (brs, 2H), 6.98 (d, J = 9.2 Hz, 2H), 7.40 (t, J = 7.2 Hz, 1H), 7.57 (t, J = 7.8 Hz, 2H), 7.67 (d, J = 7.6 Hz, 2H), 7.76 (d, J = 9.2 Hz, 2H), 9.95 (s, 1H) ppm. ^{13}C NMR (100 MHz, DMSO-d_6): δ 24.6, 47.5, 55.2, 114.3, 119.5, 121.4, 128.9, 129.4, 132.3, 137.5, 146.1, 152.9, 155.3, 164.1, 169.5 ppm. IR: ν 3456w, 3336m, 2968w, 2876m, 2833w, 1872w, 1609s, 1590s, 1565m, 1551m, 1531s, 1508s cm^{-1}. Analysis calc. ($C_{21}H_{23}N_7O{\cdot}1.3H_2O{\cdot}0.4Et_2O$): C 61.34 N 22.16 H 6.74; found: C 61.32 N 22.20 H 6.73.

6.3.30. (4*E*)-4-(Amino(phenyldiazenyl)methylene)-*N*-phenyl-2-(piperidin-1-yl)-4*H*-imidazol-5-amine (5p). Compound **1h** (0.100 g, 0.34 mmol), acetonitrile, water, triethylamine (143 μL, 1.02 mmol), piperidine (65 μL, 0.68 mmol), potassium iodide (0.011 g, 0.07 mmol). After 4 hours at 40 °C, compound **5p** was obtained pure (0.084 g; 0.21 mmol; 67%). M.p. > 186 °C (dec.). ^{1}H NMR (400 MHz, DMSO-d_6): δ 1.65 (m, 6H), 3.89 (s, 4H), 5.86 (brs, 2H), 7.08 (t, J = 7.4 Hz, 1H), 7.41 (t, J = 8.4 Hz, 2H), 7.43 (t, J = 7.2 Hz, 1H), 7.59 (t, J = 8.0 Hz, 2H), 7.70 (d, J = 7.6 Hz, 2H), 7.79 (d, J = 7.6 Hz, 2H), 10.06 (s, 1H) ppm. ^{13}C NMR (100 MHz, DMSO-d_6): δ 22.5, 23.8, 25.7, 46.4, 118.2, 121.7, 123.2, 129.3, 129.4, 129.7, 137.1, 138.8, 146.4, 153.0, 164.7, 170.4 ppm. IR: ν 3347m, 2945w, 29219w, 2850m, 1587s, 1548m, 1532s cm^{-1}. Analysis calc. ($C_{21}H_{23}N_7{\cdot}0.4KI$): C 57.34 N 22.29 H 5.27; found: C 57.18 N 21.90 H 5.04.

6.3.31. (4*E*)-4-(Amino(phenyldiazenyl)methylene)-N^2,N^2-dimethyl-*N*5-phenyl-4*H*-imidazole-2,5-diamine (5q). Compound **1h** (0.100 g, 0.34 mmol) in acetonitrile, water, triethylamine (143 μL, 1.02 mmol), dimethylamine (87 μL, 0.68 mmol), potassium iodide (0.011 g, 0.07 mmol). After 4 hours at 40 °C, compound **5q** was obtained pure (0.066 g; 0.20 mmol; 58%). M.p. > 210 °C (dec.). ^{1}H NMR (400 MHz, DMSO-d_6): δ 3.33 (s, 6H), 5.76 (brs, 2H), 7.08 (t, J = 7.4 Hz, 1H), 7.40 (t, J = 8.0 Hz, 2H), 7.43 (t, J = 6.6 Hz, 1H), 7.59 (t, J = 8.0 Hz, 2H), 7.70 (d, J = 7.2 Hz, 2H), 7.80 (d, J = 7.6 Hz, 2H), 10.01 (s, 1H) ppm. ^{13}C NMR (100 MHz, DMSO-d_6): δ 37.4, 118.1, 121.5, 123.0, 129.0, 129.2, 129.4, 137.1, 138.7, 146.2, 152.8, 164.5, 171.6 ppm. IR: ν 3308m, 2921w, 2873w, 2798w, 1615m, 1592s, 1552m, 1537s cm^{-1}. Analysis calc. ($C_{18}H_{19}N_7{\cdot}0.8H_2O{\cdot}1.3CH_3CN$): C 61.67 N 28.98 H 6.16; found (X·$0.8H_2O{\cdot}1.3CH_3CN$): C 61.89 N 29.22 H 6.23.

6.3.32. (4*E*)-4-(Amino(phenyldiazenyl)methylene)-*N*-phenyl-2-(pyrrolidin-1-yl)-4*H*-imidazol-5-amine (5r). Compound **1h** (0.100 g, 0.34 mmol), acetonitrile, water, triethylamine (143 μL, 0.96 mmol), pyrrolidine (57 μL, 0.68 mmol), potassium iodide (0.011 g, 0.07 mmol). After 4 hours at 40 °C, compound **5r** was obtained pure (0.073 g; 0.20 mmol; 59%). M.p. > 219 °C (dec.). ^{1}H NMR (400 MHz, DMSO-d_6): δ 1.98 (s, 4H), 3.75 (m, 4H), 5.75 (brs, 2H), 7.08 (t, J = 7.4 Hz, 1H), 7.40 (t, J = 8.0 Hz, 2H), 7.43 (t, J = 7.4 Hz, 1H), 7.59 (t, J = 8.0 Hz, 2H), 7.70 (d, J = 7.6 Hz, 2H), 7.81 (d, J = 7.6 Hz, 2H), 10.03 (s, 1H) ppm. ^{13}C NMR (100 MHz, DMSO-d_6): δ 24.6, 47.9, 118.1, 121.5, 122.9, 129.0, 129.2, 129.4, 137.1, 138.7, 146.3, 152.9, 164.4, 169.1 ppm. IR: ν 3338m, 3315w, 3061w, 2975w, 2867w, 1614m, 1604m, 1588s, 1534m, 1551s, 1532s cm^{-1}. Analysis calc. ($C_{20}H_{21}N_7{\cdot}0.5H_2O{\cdot}0.4Et_2O$): C 62.35 N 23.56 H 6.06; found: C 62.21 N 23.82 H 6.32.

Data availability

The data supporting this article have been included as part of the ESI.†

Conflicts of interest

There are no conflicts to declare.

Acknowledgements

This work was supported by the Portuguese Foundation for Science and Technology (FCT) in the framework of the Strategic Funding: Centro de Química da Universidade do Minho (CQ-UM) - UID/00686; Centro de Física das Universidades do Minho e do Porto (CF-UM-UP) - UID/04650; Centro Interdisciplinar de Investigação Marinha e Ambiental (CIIMAR) - UIDB/04423 and UIDP/04423; Portuguese Oncology

Institute of Porto (project no. PI86-CI-IPOP-66-2019); and National NMR Network (RNRMN) - PINFRA/22161. Access to Cluster SeARCH of UMinho is acknowledged.

References

1 K. R. Iyer, N. M. Revie, C. Fu, N. Robbins and L. E. Cowen, Treatment strategies for cryptococcal infection: challenges, advances and future outlook, *Nat. Rev. Microbiol.*, 2021, **19**, 454–466, DOI: **10.1038/s41579-021-00511-0**.

2 A. T. Jamiu, J. Albertyn, O. M. Sebolai and C. H. Pohl, Update on *Candida krusei*, a potential multidrug-resistant pathogen, *Med. Mycol.*, 2021, **59**, 14–30, DOI: **10.1093/mmy/myaa031**.

3 WHO, *WHO fungal priority pathogens list to guide research, development and public health action*, 2022, vol. 1.

4 N. Rani, A. Sharma, G. Gupta and R. Singh, Imidazoles as Potential Antifungal Agents: A Review, *Mini-Rev. Med. Chem.*, 2013, **13**, 1626–1655, DOI: **10.2174/13895575113139990069**.

5 L. F. Tietze, Domino Reactions in Organic Synthesis, *Chem. Rev.*, 1996, **96**, 115–136, DOI: **10.1021/cr950027e**.

6 T. Keijer, V. Bakker and J. C. Slootweg, Circular chemistry to enable a circular economy, *Nat. Chem.*, 2019, **11**, 190–195, DOI: **10.1038/s41557-019-0226-9**.

7 F. A. Jerca, V. V. Jerca and R. Hoogenboom, Advances and opportunities in the exciting world of azobenzenes, *Nat. Rev. Chem.*, 2022, **6**, 51–69, DOI: **10.1038/s41570-021-00334-w**.

8 P. Griefs, Vorläufige Notiz über die Einwirkung von salpetriger Säure auf Amidinitro- und Aminitrophenylsäure, *Ann. Chem. Pharm.*, 1858, **106**, 123–125, DOI: **10.1002/jlac.18581060114**.

9 H. M. D. Bandara and S. C. Burdette, Photoisomerization in different classes of azobenzene, *Chem. Soc. Rev.*, 2012, **41**, 1809–1825, DOI: **10.1039/C1CS15179G**.

10 S. Crespi, N. A. Simeth and B. König, Heteroaryl azo dyes as molecular photoswitches, *Nat. Rev. Chem.*, 2019, **3**, 133–146, DOI: **10.1038/s41570-019-0074-6**.

11 G. Hartley, The Cis-form of Azobenzene, *Nature*, 1937, **140**, 281.

12 V. Ladányi, P. Dvořák, J. Al Anshori, Ľ. Vetráková, J. Wirz and D. Heger, Azobenzene photoisomerization quantum yields in methanol redetermined, *Photochem. Photobiol. Sci.*, 2017, **16**, 1757–1761, DOI: **10.1039/c7pp00315c**.

13 A. Steinegger, O. S. Wolfbeis and S. M. Borisov, Optical Sensing and Imaging of pH Values: Spectroscopies, Materials, and Applications, *Chem. Rev.*, 2020, **120**, 12357–12489, DOI: **10.1021/acs.chemrev.0c00451**.

14 T. Stoyanova, S. Stoyanov, L. Antonov and V. Petrova, *Ammonium-Azonium Tautomerism in Some N, N-Dialkylaminoazo Dyes. Part 1: General Considerations*, 1996, vol. 31.

15 M. Dong, A. Babalhavaeji, S. Samanta, A. A. Beharry and G. A. Woolley, Red-Shifting Azobenzene Photoswitches for in Vivo Use, *Acc. Chem. Res.*, 2015, **48**, 2662–2670, DOI: **10.1021/acs.accounts.5b00270**.

16 O. Sadovski, A. A. Beharry, F. Zhang and G. A. Woolley, Spectral tuning of azobenzene photoswitches for biological applications, *Angew. Chem., Int. Ed.*, 2009, **48**, 1484–1486, DOI: **10.1002/anie.200805013**.

17 A. A. Beharry, O. Sadovski and G. A. Woolley, Azobenzene photoswitching without ultraviolet light, *J. Am. Chem. Soc.*, 2011, **133**, 19684–19687, DOI: **10.1021/ja209239m**.

18 C. Knie, M. Utecht, F. Zhao, H. Kulla, S. Kovalenko, A. M. Brouwer, *et al.*, Ortho-Fluoroazobenzenes: Visible Light Switches with Very Long-Lived Z Isomers, *Chem. – Eur. J.*, 2014, **20**, 16492–16501, DOI: **10.1002/chem.201404649**.

19 M. Dong, A. Babalhavaeji, C. V. Collins, K. Jarrah, O. Sadovski, Q. Dai, *et al.*, Near-Infrared Photoswitching of Azobenzenes under Physiological Conditions, *J. Am. Chem. Soc.*, 2017, **139**, 13483–13486, DOI: **10.1021/jacs.7b06471**.

20 S. Samanta, A. Babalhavaeji, M. X. Dong and G. A. Woolley, Photoswitching of ortho-substituted azonium ions by red light in whole blood, *Angew. Chem., Int. Ed.*, 2013, **52**, 14127–14130, DOI: **10.1002/anie.201306352**.

21 M. Dong, A. Babalhavaeji, M. J. Hansen, L. Kálmán and G. A. Woolley, Red, far-red, and near infrared photoswitches based on azonium ions, *Chem. Commun.*, 2015, **51**, 12981–12984, DOI: **10.1039/c5cc02804c**.

22 D. B. Konrad, J. A. Frank and D. Trauner, Synthesis of Redshifted Azobenzene Photoswitches by Late-Stage Functionalization, *Chem. – Eur. J.*, 2016, **22**, 4364–4368, DOI: **10.1002/chem.201505061**.

23 M. J. Hansen, M. M. Lerch, W. Szymanski and B. L. Feringa, Direct and Versatile Synthesis of Red-Shifted Azobenzenes, *Angew. Chem.,– Int. Ed.*, 2016, **55**, 13514–13518, DOI: **10.1002/anie.201607529**.

24 K. Mezgebe and E. Mulugeta, Synthesis and pharmacological activities of azo dye derivatives incorporating heterocyclic scaffolds: a review, *RSC Adv.*, 2022, **12**, 25932–25946, DOI: **10.1039/d2ra04934a**.

25 J. Calbo, C. E. Weston, A. J. P. White, H. S. Rzepa, J. Contreras-García and M. J. Fuchter, Tuning azoheteroarene photoswitch performance through heteroaryl design, *J. Am. Chem. Soc.*, 2017, **139**, 1261–1274, DOI: **10.1021/jacs.6b11626**.

26 J. N. Bull, M. S. Scholz, N. J. A. Coughlan, A. Kawai and E. J. Bieske, Monitoring Isomerization of Molecules in Solution Using Ion Mobility Mass Spectrometry, *Anal. Chem.*, 2016, **88**, 11978–11981, DOI: **10.1021/acs.analchem.6b04000**.

27 N. O. Mahmoodi, S. Rahimi and M. Pasandideh Nadamani, Microwave-assisted synthesis and photochromic properties of new azo-imidazoles, *Dyes Pigm.*, 2017, **143**, 387–392, DOI: **10.1016/j.dyepig.2017.04.053**.

28 T. A. Khattab and M. Rehan, A review on synthesis of nitrogen-containing heterocyclic dyes for textile fibers - Part 2: Fused heterocycles, *Egypt. J. Chem.*, 2018, **61**, 989–1018, DOI: **10.21608/ejchem.2018.4131.1363**.

29 V. Jelínková, A. Dellai, M. Vachtlová, M. Fecková, J. Podlesný, M. Klikar, *et al.*, Molecular azo–imidazole photoswitches: Property tuning by substitution, *J. Photochem. Photobiol., A*, 2024, **449**, 115390, DOI: **10.1016/j.jphotochem.2023.115390**.

30 A. Žula, D. Kikelj and J. Ilaš, 2-Aminoimidazoles in Medicinal Chemistry, *Mini-Rev. Med. Chem.*, 2013, **13**, 1921–1943, DOI: **10.2174/1389557511313130007**.

31 E. Li, Y. Lin, X. Wu, X. Mao, H. Kang, Y. Wen, *et al.*, Regioselective single-step synthesis of 2-aminoimidazole derivatives, *Tetrahedron Lett.*, 2019, **60**, 151122, DOI: **10.1016/j.tetlet.2019.151122**.

32 D. Dantas, A. I. Ribeiro, F. Carvalho, E. Gil-Martins, R. Silva, F. Remião, *et al.*, Red-shifted and pH-responsive imidazole-based azo dyes with potent antimicrobial activity, *Chem. Commun.*, 2023, **59**, 2791–2794, DOI: **10.1039/d3cc00372h**.

33 A. I. Ribeiro, B. Vieira, C. Alves, B. Silva, E. Pinto, F. Cerqueira, *et al.*, Halochromic Silk Fabric as a Reversible pH-Sensor Based on a Novel 2-Aminoimidazole Azo Dye, *Polymers*, 2023, **15**, 1730, DOI: **10.3390/polym15071730**.

34 A. I. Ribeiro, B. Vieira, D. Dantas, B. Silva, E. Pinto, F. Cerqueira, *et al.*, Synergistic Antimicrobial Activity of Silver Nanoparticles with an Emergent Class of Azoimidazoles, *Pharmaceutics*, 2023, **15**, 926, DOI: **10.3390/pharmaceutics15030926**.

35 A. C. Serra, C. Docal and A. M. d'A. Rocha Gonsalves, Efficient azo dye degradation by hydrogen peroxide oxidation with metalloporphyrins as catalysts, *J. Mol. Catal. A: Chem.*, 2005, **238**, 192–198, DOI: **10.1016/j.molcata.2005.05.017**.

36 A. Malloum, J. J. Fifen and J. Conradie, Determination of the absolute solvation free energy and enthalpy of the proton in solutions, *J. Mol. Liq.*, 2021, **322**, 114919, DOI: **10.1016/j.molliq.2020.114919**.

37 F. Neese, Software update: The ORCA program system—Version 5.0, *Wiley Interdiscip. Rev.: Comput. Mol. Sci.*, 2022, **12**, e1606, DOI: **10.1002/wcms.1606**.

38 F. Weigend and R. Ahlrichs, Balanced basis sets of split valence, triple zeta valence and quadruple zeta valence quality for H to Rn: Design and assessment of accuracy, *Phys. Chem. Chem. Phys.*, 2005, **7**, 3297, DOI: **10.1039/b508541a**.

39 F. Neese, An improvement of the resolution of the identity approximation for the formation of the Coulomb matrix, *J. Comput. Chem.*, 2003, **24**, 1740–1747, DOI: **10.1002/jcc.10318**.

40 F. Weigend, Accurate Coulomb-fitting basis sets for H to Rn, *Phys. Chem. Chem. Phys.*, 2006, **8**, 1057, DOI: **10.1039/b515623h**.

41 E. Caldeweyher, S. Ehlert, A. Hansen, H. Neugebauer, S. Spicher, C. Bannwarth, *et al.*, A generally applicable atomic-charge dependent London dispersion correction, *J. Chem. Phys.*, 2019, **150**, 154122, DOI: **10.1063/1.5090222**.

42 H. Kruse and S. Grimme, A geometrical correction for the inter- and intra-molecular basis set superposition error in Hartree-Fock and density functional theory calculations for large systems, *J. Chem. Phys.*, 2012, **136**, 154101, DOI: **10.1063/1.3700154**.

43 A. I. Ribeiro, C. Gabriel, F. Cerqueira, M. Maia, E. Pinto, J. C. Sousa, *et al.*, Synthesis and antimicrobial activity of novel 5-aminoimidazole-4-carboxamidrazones, *Bioorg. Med. Chem. Lett.*, 2014, **24**, 4699–4702, DOI: **10.1016/j.bmcl.2014.08.025**.